In Vitro Cell.Dev.Biol.—Animal (2012) 48:143–148
DOI 10.1007/s11626-012-9486-z

REPORT

Mouse ES cells maintained in different pluripotency-promoting conditions differ in their neural differentiation propensity

Haruka Hirose · Hidemasa Kato · Akie Kikuchi-Taura · Toshihiro Soma · Akihiko Taguchi

Received: 23 November 2011 / Accepted: 8 January 2012 / Published online: 27 January 2012 / Editor: T. Okamoto

Abstract Prior to differentiation, embryonic stem (ES) cells in culture are maintained in a so-called "undifferentiated" state, allowing derivation of multiple downstream cell lineages when induced in a directed manner, which in turn grants these cells their "pluripotent" state. The current work is based on a simple observation that the initial culture condition for maintaining mouse ES cells in an "undifferentiated" state does impact on the differentiation propensity of these cells, in this case to a neuronal fate. We point out the importance in judging the "pluripotency" of a given stem cell culture, as this clearly demonstrated that the "undifferentiated" state of these cells is not necessarily a "pluripotent" state, even for a widely used mouse ES cell line. We partly attribute this difference in the initial value of ES cells to the naïve-to-primed status of pluripotency, which in turn may affect early events of the differentiation in vitro.

Keywords Embryonic stem cell · Culture media · Naïve · Primed · *Fgf5*

H. Hirose · A. Kikuchi-Taura · A. Taguchi
Department of Regenerative Medicine,
National Cerebral and Cardiovascular Center,
5-7-1 Fujishiro-dai,
Suita, Osaka, Japan 565-8565

H. Kato (✉)
Division of Developmental Biology, Research Center for Genomic Medicine, Saitama Medical University,
1397-1 Yamane,
Hidaka, Saitama, Japan 350-1241
e-mail: hidekato@saitama-med.ac.jp

T. Soma
Division of Hematology, Department of Internal Medicine,
Hyogo College of Medicine,
1-1 Mukogawachou,
Nishinomiya, Hyogo, Japan 663-850

A. Taguchi
Department of Regenerative Medicine Research,
Institute of Biomedical Research and Innovation,
2-2 Minatojima Minamimachi Chuo-ku,
Kobe, Hyogo, Japan 650-0047

Introduction

The use of embryonic stem (ES) cells has spread from a classical tool for gene targeting toward models whereby we can test their in vitro developmental properties (in a hope to be reproduced in human systems) for potential therapeutic uses. Previously, the ultimate task for mouse ES cells was to commit into the germ cell lineage when implanted into blastocysts in order to produce transgenic animals. However, the current favorable destinations have been widened up to cells of various organs including brain, heart, pancreas, liver, and many more because of the anticipation toward regenerative medicine. As a consequence, the fashion and requirements to maintain "pluripotent" ES cells are to be modified. Also, if these cells are considered to be directly transplanted into human host organs, concerns naturally rise to avoid animal-derived components (such as mouse feeder cells or bovine serum). To this purpose, a number of serum-free/chemically defined media has been developed from various groups (Furue et al. 2005; Tsuji et al. 2008; Chen et al. 2011).

ES cells are artificial cell entities trapped in a "quasi-eternal" moratorium state for development. In the case of mouse ES cells, this characteristic is mainly endowed by leukemia inhibitory factor (LIF) through its STAT3-activating property (Matsuda et al. 1999). Also, LIF is acting to inhibit MAP kinase activation, which is known to be necessary for the successive development to occur (Hirai et al. 2011). This cell state in which ES cells are

stabilized for self-renewal is now understood as the "ground state" (Ying et al. 2008). The cells in this ground state are considered to be "naïve" (Nichols and Smith 2009) as they are refractory to spontaneous differentiation and self-renew (Ying et al. 2008) without any requirement of mitogen. In contrast, upon LIF removal, ES cells are expected to be swiftly primed for differentiation, a condition also coined "primed" by Smith and colleagues (Nichols and Smith 2009). A suitable condition for ES cell culture is therefore to stably maintain the naïve state during cell expansion but be able to swiftly switch to a primed condition when needed. To date, however, a prospective evaluation of this "switch ability" has not been reported.

Recently, it has been shown that this ground state varies among different mouse strains. It is now considered that the often-used 129 mouse background to derive ES cells has an exceptional property to create a stable ground state (Suzuki et al. 1999). In other strains of mice, this ground state is inherently less stable and hence is now called metastable (Hanna et al. 2009), which explains the difference in the efficiency in deriving ES cell lines from various mouse genetic backgrounds (Suzuki et al. 1999).

We have previously reported a highly reproducible neural induction protocol for mouse ES cells (Bouhon et al. 2005, 2006), which fits well the proposed developmental model of "default neurogenesis" (Hemmati-Brivanlou and Melton 1997; Chang and Hemmati-Brivanlou 1998) originally described for amphibians.

Our study provides evidence that quality control of ES cells for their pluripotency can be only achieved through the incorporation of developmental stage evaluation, especially vis-à-vis the ground state, and also that it may vary according to the aimed cell lineage.

Materials and methods

ES cell culture. Throughout this study, we have used a mouse ES cell line CMTI-1, derived from 129svev mouse background, known to be relatively less dependent to mouse embryonic fibroblast (MEF) feeder cells. However, for the routine maintenance of these cells, the cultures were performed on MEF feeder layer to ensure their pluripotency. ES cells were cultured in Dulbecco's modified eagle medium containing 15% fetal bovine serum (FBS), 1,000 U/ml leukemia inhibitory factor (LIF; Millipore, Billerica, MA), 100 μM 2-mercaptoethanol, 0.03% L-glutamine, 1 mM sodium pyruvate, 100 μM non-essential amino acid, 50 U/ml penicillin, and 50 μg/ml streptomycin (ES cell medium). We routinely split ES cells every other day and replate them at 2.4×10^6 cells/100-mm gelatinized-culture dish. ES cells were gently dispersed using 0.01% trypsin/0.1 mM EDTA in PBS at room temperature by triturating using pipettes. After neutralizing trypsin activity, the cells were collected by centrifugation and resuspended in a fresh medium before plating. To convert from serum-supplemented (SS) to serum-free (SF) media, we adopted the method of "sequential adaptation" suggested by the manufacturer of a widely used compound which substitutes serum in the culture of ES cells, Knockout Serum Replacement (KSR; Invitrogen, Carlsbad, CA) which is also used in the current study or ESFC (Cell Science and Technology Institute, Inc., Tokyo, Japan; Furue et al. 2005). These media were also supplemented with 1,000 U/ml LIF.

Our serum-free adaptation culture steps comprise of starting from a completely serum-supplemented medium, culture media were diluted out using each non-serum media by ratios as follows; Serum media : non-serum media=1:0 (zeroth passage), 3:1 (first passage), 1:1 (second passage), 1:3 (third passage), 1:9 (fourth passage), and ultimately to completely non-serum media (fifth passage onward).

RT-PCR. Total RNA was purified from cells harvested at indicated time points by using RNeasy Micro Kit (QIAGEN, the Netherlands). One microgram of total RNA was used for reverse transcription reaction with Omniscript Reverse Transcriptase (QIAGEN) and Oligo-dT Primer (Invitrogen).

PCR was carried out with TaKaRa Ex Taq Hot Start Version (TaKaRa, Shiga, Japan) and primers listed in Table 1. Each reaction was performed according to manufacturer's protocol. PCR products were electrophoresed in agarose gel and visualized by ethidium bromide.

Induction of neural progenitors from ES cells. SF/feeder-free-adapted ES cells were trypsinized and then neural induction was performed in non-adherent dishes in Chemically Defined Medium (CDM) as described previously (Bouhon et al. 2005, 2006). CDM is a non-instructive developmentally neutral medium consisting of Iscove's Modified Dulbecco's Medium, Ham's F-12 containing polyvinyl alcohol (final concentration 0.1%), holo-transferrin, 1-thioglycerol, insulin, GlutaMAX and a mixture of chemically defined lipids. Suspended cells formed aggregates and were collected and analyzed at day 8 of differentiation when the aggregates contain neural progenitors and some neurite-extending mature neurons. A minor modification to our reported paper is the inclusion of a cell dissociation step at day 4 using Accumax to reduce cell heterogeneity.

Results

Serum-free, feeder-free adaptation culture of ES cells. Commercially available 129svev-derived mouse ES cells (CMTI-1), which can be stably maintained in a serum-containing medium under a non-feeder condition, were used

Table 1. RT-PCR primers used in this study

Gene	Forward primer	Reverse primer
Oct3/4	GGCTTCAGACTTCGCCTCC	AACCTGAGGTCCACAGTATGC
Nanog	TCTTCCTGGTCCCCACAGTTT	GCAAGAATAGTTCTCGGGATGAA
Zfp42/Rex 1	CCCTCGACAGACTGACCCTAA	TCGGGGCTAATCTCACTTTCAT
Fgf5	TGTGTCTCAGGGGATTGTAGG	AGC TGTTTTCTTGGAATCTCTC C
Nestin	CCCTGAAGTCGAGGAGCTG	CTGCTGCACCTCTAAGCGA
Musa.shi	CCTCTCACGGCTTATGGGC	CTGTGGCAATCAAGGGACC
Neurogenin2	AAC TCCACGTCC CCATACAG	GAGGCG CATAACGATGCTTCT
Gata6	ACCTTATGGC GTAGAAAT GC TGAGGGTG	C TGAAJAC TTGAGGTCACTGTTCTCGGG
Kff4	CC GGC GGGAAGGGAGAAGACAC TGCGT	GTGGGTTAGCGAGTTGGAAAGGATAAA
NeuroD 1	CGCCTACAGCGCAGCTCTGG	CGTCGCTGCAGGGTAGTGCA
Ascli	GCTGCAAACGCCGGCTCAAC	GCGGATGTACTCGACCGCCG
Dkk 1	GTCCAAGATCTGTAAACC	GAGTCAAGACAATCAACC
Actb	GGCTGTATTCCCCTCCATCG	CCAGTTGGTAACAATGCCATGT
Gapdh	AGGTC GGTGTGAACGGATTTG	TGTAGAC CATGTAGTTGAGGTCA

throughout the study. To enable direct comparison of the neural differentiation propensities of the same ES cells maintained in different pluripotency-promoting conditions, mouse ES cells cultured under serum-containing medium condition (which represents a routine lab culture condition) were parallely adapted toward two non-serum culture conditions (C-KSR and C-ESFC) as depicted in Fig. 1*a*. From a single ES cell-confluent mouse embryonic fibroblasts (MEF)-fed culture dish in serum-containing media, the two conditions were processed in parallel for ES cell propagation. In Fig 1*a*, C-KSR and C-ESFC depict the sequential adaptation conditions to the KSR-supplemented and ESFC

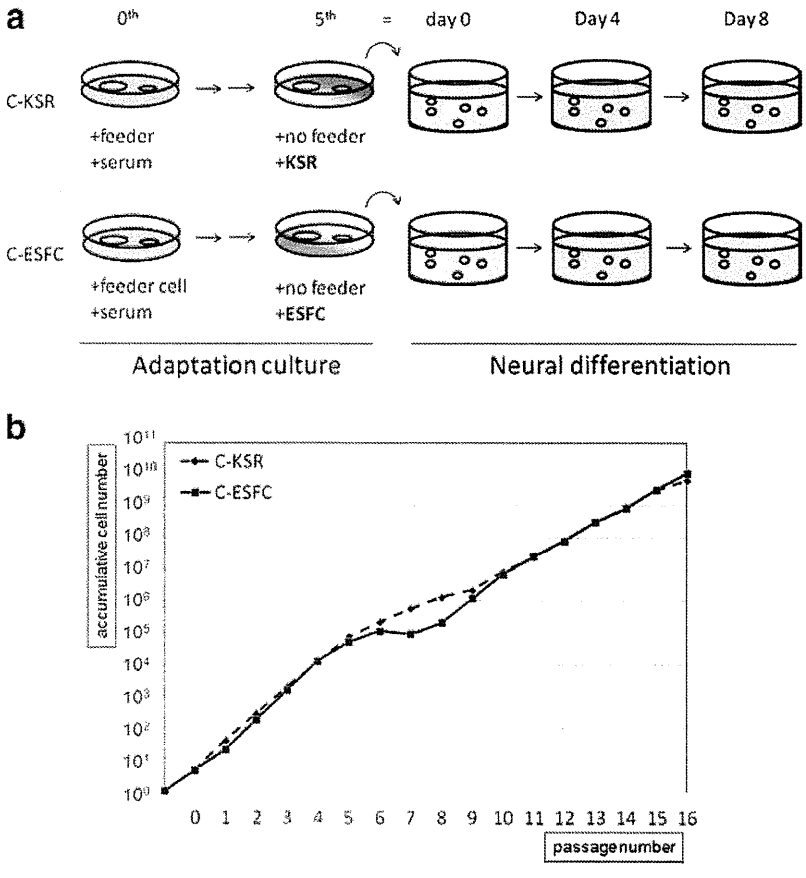

Figure 1. (*a*) Schematic drawing of our experiment depicting the parallel adaptation procedure followed by neural differentiation. Starting from a single MEF feeder ES cell dish (zeroth), cultures were serially adapted in parallel to non-serum medium with KSR (C-KSR) or ESFC (C-ESFC). At the fifth passage, cultures are completely serum-free and were subjected to differentiation into neural progenitor cells. (*b*) A representative cell growth profile during prolonged cell cultures in either KSR or ESFC. Cell proliferation rate as well as cell morphology (data not shown) did not change significantly between condition C-KSR and C-ESFC indicating that both media sustain ES cell self-renewal for a long culture period.

SF media, respectively. As hinted by its manufacturer and observed elsewhere, we found difficulties in efficiently propagating ES cells when the culture was directly transferred into the KSR medium without the adaptation steps probably due to "culture shock" (data not shown). After five passages, both groups were considered to be "adapted" as the culture media are then completely converted to serum-free conditions and virtually no residual MEFs have been observed (see "Materials and methods" for details). All conditions were with leukemia inhibitory factor (LIF; ESGRO; Millipore) at 1,000 unit/mL.

Figure 1*b* shows representative growth profiles of the ES cells under the two culture conditions. Both culture media maintained ES cell proliferation for at least 16 passages (Fig. 1*b*) without any sign of overt differentiation judged by microscopic observation. Both groups showed comparative growth rates throughout the adaptation culture procedure. Interestingly, a combined effect of the serum-containing and SF medium on cell proliferation has been observed (approximately in the fifth passage). This is in good accordance with the idea that the factors supplemented in each SF medium, provides independent mechanisms for ES cell growth (which cannot be substituted at least with factors present in the serum used in this study). Although cell and colony morphology was largely similar between C-KSR- and C-ESFC-cultured cells (Fig. 1*b*), we found a tendency for C-ESFC-cells to form "domed" colonies.

We therefore concluded at this step that the two culture conditions used in this study are comparable for their cell proliferative capacities.

Comparative analyses of the pluripotency markers in undifferentiated ES cells. To comparatively analyze the pluripotency of the ES cells under the two different conditions, the expression levels of classical pluripotency markers, that are *Pou5f1* (also called *Oct-3/4*), *Nanog*, *Klf4*, *Zfp42* (also called *Rex1*), were evaluated. These transcription factors have been repeatedly shown to be essential for the pluripotency of the ES cells by creating a core transcriptional network (Kim et al. 2008). RT-PCR analyses showed no obvious difference in the expression levels of core pluripotency factors *Pou5f1*, *Sox2*, and *Nanog* before differentiation (KSR D0 and ESFC D0 columns in Fig. 2). However, we found significant differences for the expression of *Zfp42*, and *Klf4* (Fig. 2). As the latter two markers are representative for naïve ES cells (Nichols and Smith 2009), we next turn our attention to a primitive ectoderm marker, *Fgf5*, which can discriminate the two distinct states of ES cells, which are naïve versus primed. By semi-quantitative RT-PCR, we observed that ES cells in the C-ESFC have significantly higher level of *Fgf5* expression before differentiation (Fig. 2). Judging by these results, we

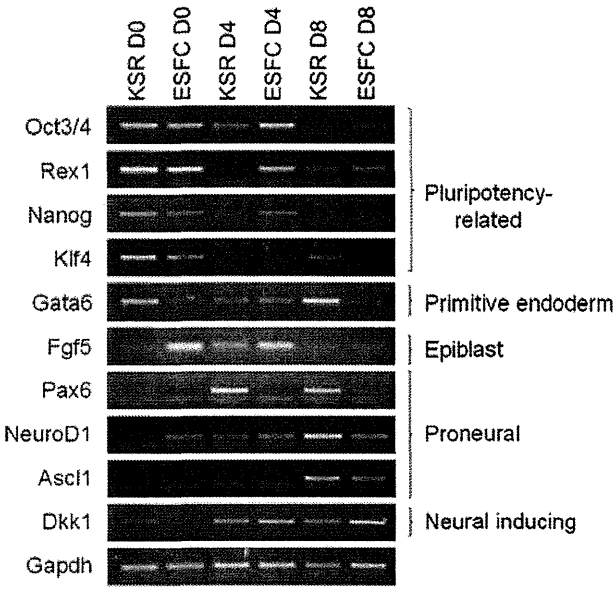

Figure 2. Developmentally regulated gene expression during the parallel differentiation of ES cells maintained either in KSR- or ESFC-media. At the start of differentiation (D0), pluripotency-related markers (*Nanog*, *Rex1*, *Oct3/4*, and *Klf4*) were both positive under condition C-KSR and C-ESFC. Major differences in marker expression at this undifferentiated stage were observed for a primitive endodermal marker *Gata6* and for a primitive ectoderm/epiblast marker *Fgf5*. At D4 of differentiation, pluripotency-related factor's expression (Oct3/4, Rex1, and Nanog) persisted only in ESFC-derived cells which may signify a delayed differentiation or a residual population of undifferentiated cells. Interestingly, an early neuroectodermal marker *Pax6* was only turned on from KSR-cells. Consistently, at D8 of differentiation when the majority of cells within the differentiating spheres are expected to be of neural characters (Bouhon et al. 2005), only KSR-derived cells expressed *Pax6* as well as other proneural markers such as *NeuroD1* and *Ascl1*. The gene expression levels for the neural-inducing agent Dkk1 were even for both groups if not higher for the neural-recalcitrant ESFC-derived cells.

tentatively interpret that culture condition C-KSR tends to maintain ES cells in a naïve state compared to C-ESFC condition, which in turn seems to retain these cells in a more primed state.

Naïve-to-primed balance impacts on the neural induction efficiency of ES cells. A strong motivation which led us to this current study was our empirical observation that neural induction starting from mouse ES cells highly depended on the initial undifferentiated state of the culture. Even mouse ES cells with less dependency on feeder cells, such as 129Ola- or 129svev-derived ES cells, exhibit abnormal morphologies upon prolonged culture. This was observed without necessarily changing their expression profiles for the pluripotency-related markers such as *Oct3/4*, *Sox2* or *Nanog* (data not shown). We knew that this tendency was almost always accompanied with poor differentiation outputs. We

therefore reasoned that ES cell properties apart from the core pluripotency factors' statuses would influence such differentiation propensities. To this end, we in vitro differentiated in parallel, ES cells cultured either in condition C-KSR or C-ESFC (remaining columns in Fig. 2). The differentiation protocol we have independently developed has a characteristic similar to the "default model" of early embryonic cell differentiation (Chang and Hemmati-Brivanlou 1998; see "Discussion"). As shown in Fig. 2, we observed a distinct transcriptional regulation for *Pax6*, which is an early marker for our default neural progenitor cells (Bouhon et al. 2006). In addition, the proneural genes *NeuroD1* and *Ascl1* (also called *Mash1*) showed strongly biased expression in favor of C-KSR-derived cells. In addition, *Musashi1* and *Neurogenin2* also showed similar tendencies (data not shown). When we turn our attention to the pluripotency-related markers, we surprisingly found that C-ESFC condition exhibits a resistance for this differentiation judging by residual expression of *Pou5f1*, *Nanog*, *Rex1*, and *Fgf5* (see for examples, expression levels of *Pou5f1* and *Nanog* in ESFC D4 samples).

It is also noteworthy that the neural-inducing activities of *Dkk1*, an antagonist of Wnt activity expressed from a non-neural cell lineage transiently present in our differentiation culture, seem comparable between the two groups in terms of expression level and/or timing.

Discussion

Hochedlinger and coworkers have pinpointed epigenetic alterations which impair induced pluripotent stem (iPS) cells from their full developmental potentials (Stadtfeld et al. 2010). Surprisingly, they have spotted a gene locus which is governed by genetic imprinting but with no implication to pluripotency. This represents a good example implying that the "superficial" pluripotency, judged by expression of restricted number of markers is not sufficient to predict full developmental potential.

In this work, we have observed that the expressivity of *Fgf5* could serve for such a predictive marker for developmental potential, at least to a neural cell lineage, provided that the core pluripotency markers (*Pou5f1*, *Sox2*, and *Nanog*) are present. *Fgf5* is exclusively expressed in epiblast and in epiblast stem cells which are derived from it (Pelton et al. 2002). However, in a recent work, its expression has also been demonstrated in cells at their "primed" state for differentiation (Nichols and Smith 2009). This indicates that the differentiation efficiency using a specific induction protocol is influenced by not only the superficial pluripotent state but also the different degree of "priming" for differentiation. Our current study is indicative that this variety of differentiation priming is a consequence of the culture environment, in this case, the culture media, as all other conditions have been equalized. In the future, it would therefore be necessary to manipulate the cell culture system of ES cell, prior to its differentiation, according to the aimed cell lineage. To this end, the effort presented in this work should also be extended for other cell lineages than neural.

The reason why a "primed-like" condition (C-ESFC) was more refractory to neural differentiation would warrant further investigation. Our previous observation in which we showed that a transient contribution of primitive endoderm lineage was present during this neural differentiation might explain this puzzling situation. As *Fgf5* expression is suggestive that the cells are more committed toward an epiblast-like stage, high expressors of *Fgf5* may be more recalcitrant to produce primitive endoderm lineage cells, which segregate earlier during development from epiblast primitive ectoderm (Lu et al. 2001). Although *Dkk1* which is mainly expressed from the anterior visceral endoderm, a descendant of the primitive endoderm, is equally expressed in both conditions during differentiation, the possibility that the neural-inducing cell populations differ between the two groups merits further investigation. An important observation of our study is that markers which are indicative of an undifferentiated state of ES cells disappeared more slowly in C-ESFC. Because the primed state in the developmental context signifies its readiness to differentiate, this cannot be easily reconciled with the idea that C-ESFC is more "primed" or more advanced in the developmental schedule (judged by *Fgf5* expression). This implication that the cells in a certain condition do not enter the neural fate within the due duration of the experiment could be because of delayed lineage choice or because the cells have entered a distinct state from which they cannot reach the neural fate. This observation would warrant deeper investigation in the future if one is to prospectively judge the developmental propensities of a given stem cell line or to evaluate and determine the proper initial characteristics of the iPS cells generated.

At the very least, our finding is suggestive that most cell differentiation protocols are highly sensitive to a subtle difference in the developmental stages of ES cells which cannot be easily standardized if the culture conditions of ES cells differ from lab to lab. This may also explain the encountered difficulties in reproducing cell differentiation protocols by different labs.

Acknowledgments H. K. thanks Nick Allen for sharing unpublished data related to the neural differentiation protocol and for the long-term friendship. We all thank Yosuke Moriyama for critically reading the manuscript. This work was supported by Grants-in-Aid for Scientific Research on Innovative Areas (KAKENHI 23111008) awarded to H. K.

References

Bouhon I. A.; Joannides A.; Kato H.; Chandran S.; Allen N. D. Embryonic stem cell-derived neural progenitors display temporal restriction to neural patterning. *Stem Cells* 24: 1908–1913; 2006.

Bouhon I. A.; Kato H.; Chandran S.; Allen N. D. Neural differentiation of mouse embryonic stem cells in chemically defined medium. *Brain Res. Bull.* 68: 62–75; 2005.

Chang C.; Hemmati-Brivanlou A. Cell fate determination in embryonic ectoderm. *J. Neurobiol.* 36: 128–151; 1998.

Chen G.; Gulbranson D. R.; Hou Z.; Bolin J. M.; Ruotti V.; Probasco M. D.; Smuga-Otto K.; Howden S. E.; Diol N. R.; Propson N. E.; Wagner R.; Lee G. O.; Antosiewicz-Bourget J.; Teng J. M.; Thomson J. A. Chemically defined conditions for human iPSC derivation and culture. *Nat. Methods* 8: 424–429; 2011.

Furue M.; Okamoto T.; Hayashi Y.; Okochi H.; Fujimoto M.; Myoishi Y.; Abe T.; Ohnuma K.; Sato G. H.; Asashima M.; Sato J. D. Leukemia inhibitory factor as an anti-apoptotic mitogen for pluripotent mouse embryonic stem cells in a serum-free medium without feeder cells. *In Vitro Cell. Dev. Biol. Anim.* 41: 19–28; 2005.

Hanna J.; Markoulaki S.; Mitalipova M.; Cheng A. W.; Cassady J. P.; Staerk J.; Carey B. W.; Lengner C. J.; Foreman R.; Love J.; Gao Q.; Kim J.; Jaenisch R. Metastable pluripotent states in NOD-mouse-derived ESCs. *Cell Stem Cell* 4: 513–524; 2009.

Hemmati-Brivanlou A.; Melton D. Vertebrate neural induction. *Annu. Rev. Neurosci.* 20: 43–60; 1997.

Hirai H.; Karian P.; Kikyo N. Regulation of embryonic stem cell self-renewal and pluripotency by leukaemia inhibitory factor. *Biochem. J.* 438: 11–23; 2011.

Kim J.; Chu J.; Shen X.; Wang J.; Orkin S. H. An extended transcriptional network for pluripotency of embryonic stem cells. *Cell* 132: 1049–1061; 2008.

Lu C. C.; Brennan J.; Robertson E. J. From fertilization to gastrulation: axis formation in the mouse embryo. *Curr. Opin. Genet. Dev.* 11: 384–392; 2001.

Matsuda T.; Nakamura T.; Nakao K.; Arai T.; Katsuki M.; Heike T.; Yokota T. STAT3 activation is sufficient to maintain an undifferentiated state of mouse embryonic stem cells. *EMBO J.* 18: 4261–4269; 1999.

Nichols J.; Smith A. Naive and primed pluripotent states. *Cell Stem Cell* 4: 487–492; 2009.

Pelton T. A.; Sharma S.; Schulz T. C.; Rathjen J.; Rathjen P. D. Transient pluripotent cell populations during primitive ectoderm formation: correlation of in vivo and in vitro pluripotent cell development. *J. Cell Sci.* 115: 329–339; 2002.

Stadtfeld M.; Apostolou E.; Akutsu H.; Fukuda A.; Follett P.; Natesan S.; Kono T.; Shioda T.; Hochedlinger K. Aberrant silencing of imprinted genes on chromosome 12qF1 in mouse induced pluripotent stem cells. *Nature* 465: 175–181; 2010.

Suzuki O.; Matsuda J.; Takano K.; Yamamoto Y.; Asano T.; Naiki M.; Kusanagi M. Effect of genetic background on establishment of mouse embryonic stem cells. *Exp. Anim.* 48: 213–216; 1999.

Tsuji Y.; Yoshimura N.; Aoki H.; Sharov A. A.; Ko M. S.; Motohashi T.; Kunisada T. Maintenance of undifferentiated mouse embryonic stem cells in suspension by the serum- and feeder-free defined culture condition. *Dev. Dyn.* 237: 2129–2138; 2008.

Ying Q. L.; Wray J.; Nichols J.; Batlle-Morera L.; Doble B.; Woodgett J.; Cohen P.; Smith A. The ground state of embryonic stem cell self-renewal. *Nature* 453: 519–523; 2008.

Cell Death and Differentiation (2012) 19, 756–767

www.nature.com/cdd

Open

Glucocorticoid-induced TNF receptor-triggered T cells are key modulators for survival/death of neural stem/progenitor cells induced by ischemic stroke

M Takata[1,3,5], T Nakagomi[1,5], S Kashiwamura[2,5], A Nakano-Doi[1], O Saino[1], N Nakagomi[1], H Okamura[2], O Mimura[3], A Taguchi[4] and T Matsuyama*[,1]

Increasing evidences show that immune response affects the reparative mechanisms in injured brain. Recently, we have demonstrated that CD4$^+$T cells serve as negative modulators in neurogenesis after stroke, but the mechanistic detail remains unclear. Glucocorticoid-induced tumor necrosis factor (TNF) receptor (GITR), a multifaceted regulator of immunity belonging to the TNF receptor superfamily, is expressed on activated CD4$^+$T cells. Herein, we show, by using a murine model of cortical infarction, that GITR triggering on CD4$^+$T cells increases poststroke inflammation and decreases the number of neural stem/progenitor cells induced by ischemia (iNSPCs). CD4$^+$GITR$^+$T cells were preferentially accumulated at the postischemic cortex, and mice treated with GITR-stimulating antibody augmented poststroke inflammatory responses with enhanced apoptosis of iNSPCs. In contrast, blocking the GITR–GITR ligand (GITRL) interaction by GITR–Fc fusion protein abrogated inflammation and suppressed apoptosis of iNSPCs. Moreover, GITR-stimulated T cells caused apoptosis of the iNSPCs, and administration of GITR-stimulated T cells to poststroke severe combined immunodeficient mice significantly reduced iNSPC number compared with that of non-stimulated T cells. These observations indicate that among the CD4$^+$T cells, GITR$^+$CD4$^+$T cells are major deteriorating modulators of poststroke neurogenesis. This suggests that blockade of the GITR–GITRL interaction may be a novel immune-based therapy in stroke.
Cell Death and Differentiation (2012) **19,** 756–767; doi:10.1038/cdd.2011.145; published online 4 November 2011

Brain injury induces acute inflammation, thereby exacerbating poststroke neuronal damage.[1–4] Although central nervous system (CNS) is known for its limited reparative capacity, inflammation is a strong stimulus for reparative mechanisms including activation of neurogenesis. However, the latter results in low survival of newly generated neural stem cells.[5] These findings indicate the relevance of endogenous regulatory and/or environmental factors for survival and differentiation of neural stem cells.

In a murine model of cerebral ischemia, we have detected neural stem/progenitor cells induced by ischemia (ischemia-induced neural stem/progenitor cells; iNSPCs) in the post-stroke cerebral cortex.[6] More recently, we have observed spontaneous accelerated repair in severe combined immunodeficient mice (SCID) compared with immunocompetent wild-type controls,[7] and have demonstrated that CD4$^+$T cells serve as negative regulators in the survival of iNSPCs.[8] Together with previous reports supporting the importance of the role of T cells in regulating poststroke inflammation[1,2,9] and functional recovery,[1,10,11] these findings emphasize on the link between CD4$^+$T cells and survival of iNSPCs. However, the mechanistic details and the subpopulation of CD4$^+$T cells responsible for acting as negative regulators in CNS repair remain unclear.

Glucocorticoid-induced tumor necrosis factor (TNF) receptor (GITR)-related protein that was originally cloned in a glucocorticoid-treated hybridoma T-cell line[12] is a protein belonging to the TNF receptor superfamily. It is expressed at basal levels in responder resting T cells, with CD4$^+$T cells including CD4$^+$CD25$^+$T cells (regulatory T cell, Treg) having a higher GITR expression than CD8$^+$T cells.[13] When the T cells are activated, GITR is strongly upregulated in responder CD4$^+$T cells. In this situation, the stimulatory effect of responder T cells was more activated[13,14] and the suppressing effect of Treg was completely abrogated,[13] leading to a more enhanced immune/inflammatory response.[15] In the CNS, it has been reported that blocking of the GITR–GITR ligand (GITRL) interaction protected spinal cord injury from

[1]Laboratory of Neurogenesis and CNS Repair, Hyogo College of Medicine, 1-1 Mukogawacho, Nishinomiya, Hyogo 663-8501, Japan; [2]Laboratory of Self Defense, Institute for Advanced Medical Sciences, Hyogo College of Medicine, 1-1 Mukogawacho, Nishinomiya, Hyogo 663-8501, Japan; [3]Department of Ophthalmology, Hyogo College of Medicine, 1-1 Mukogawacho, Nishinomiya, Hyogo 663-8501, Japan and [4]Department of Cerebrovascular Disease, National Cardiovascular Research Center, Osaka 565-8565, Japan

*Corresponding author: T Matsuyama, Laboratory of Neurogenesis and CNS Repair, Institute for Advanced Medical Sciences, Hyogo College of Medicine, 1-1 Mukogawacho, Nishinomiya, Hyogo 663-8501, Japan. Tel: +81 798 45 6821; Fax: +81 798 45 6823; E-mail: tomohiro@hyo-med.ac.jp

[5]These authors contributed equally to this work.

Keywords: GITR; Fas; T-cell; neural stem cell; ischemia

Abbreviations: BrdU, 5-bromo-2′-deoxyuridine; CNS, central nervous system; DAPI, 4′,6-diamino-2-phenylindole; EGF, epidermal growth factor; FasL, Fas ligand; GAPDH, glyceraldehyde-3-phosphate dehydrogenase; GITR, glucocorticoid-induced tumor necrosis factor receptor; GITRL, GITR ligand; GFP, green fluorescent protein; gld, generalized lymphoproliferative disorder = spontaneous mutation in the Fas ligand gene; iNSPC, ischemia-induced neural stem/progenitor cell; MCA, middle cerebral artery; SCID, severe combined immunodeficient; Sox2, SRY (sex determining region Y)-box 2; TCR, T-cell receptor; Treg, regulatory T cell

Received 23.5.11; revised 06.9.11; accepted 27.9.11; Edited by JA Cidlowski; published online 04.11.11

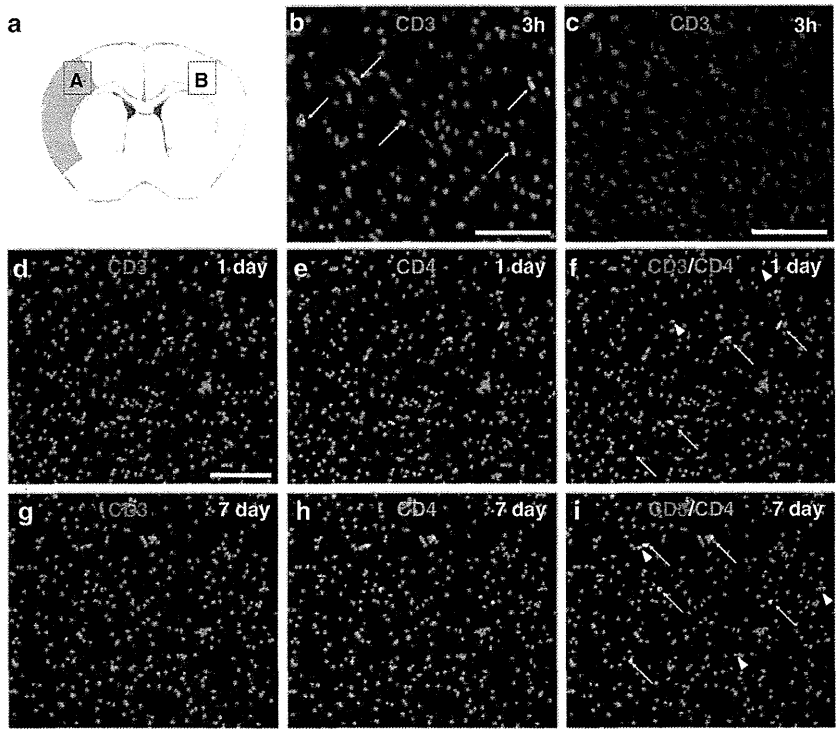

Figure 1 T-cell infiltration into the ischemic area of the poststroke brain. Immunohistochemistry for $CD3^+$ cells (T cells; (**a**) B: ischemic area and C: contralateral cortex) and $CD4^+$T cells (**d–i**) infiltrated into the postischemic cortex 3 h (**b** and **c**), 1 day (**d**) and 7 days (**g**) after stroke. $CD3^+$ T cells were positive for CD4 1 day and 7 days (arrows, **d** and **g**: CD3; **e** and **h**: CD4; **f** and **i**: merged, nuclei were counterstained with DAPI) after stroke. Arrowheads indicate $CD4^-$ T cells (**f** and **i**). (**b–i**) Scale bar: 100 μm

the inflammatory response,[16] whereas GITR triggering worsened experimental autoimmune encephalomyelitis while stimulating autoreactive $CD4^+$T cells.[17] These observations lead us to hypothesize that GITR triggering on T cells may serve as a negative regulator for CNS repair after cerebral infarction.

In this study, we demonstrated for the first time that GITR triggering on T cells following ischemic stroke enhanced poststroke inflammation and cell death of iNSPCs. Administration of GITR–Fc fusion protein markedly suppressed these responses. In addition, GITR-triggered T cells directly induced apoptosis of iNSPCs *in vitro*. Our current results show that activated $GITR^+$T cells acted as negative modulators for CNS restoration, indicating that blockade of the GITR–GITRL interaction can be a novel strategy for treating ischemic stroke.

Results

Infiltration of $CD4^+GITR^+$T cells into the ischemic cortex after stroke. Immunohistochemistry (Figures 1a–c) revealed that $CD3^+$ cells (T cells) appeared to infiltrate the ischemic region as early as 3 h after stroke (Figure 1b) and were observed continuously during the poststroke period (Figures 1d and g). The T cells were rarely observed at nonischemic ipsilateral or contralateral cortex (Figure 1c). Most T cells in the ischemic region (~70% of T cells) were CD4 positive (Figures 1d–i), indicating that $CD4^+$T cells predominantly infiltrate the poststroke cortex. However, GITR-positive cells were not found in the ischemic region at 6 h after stroke (Figure 2a), whereas a number of T cells were detected at the same region (Figures 2b and c). This indicates that GITR was not expressed in the infiltrated T cells at early poststroke period. GITR-expressing cells started to appear at 24 h after stroke and gradually increased in number. At 7 days post stroke, a number of $CD3^+$T cells co-express GITR (Figures 2d–f). Calculating the number of infiltrated T cells in serial brain sections revealed that ~65% of $CD4^+$T cells were GITR positive, indicating that $GITR^+$ T cells predominantly occupied the subset of $CD4^+$T cells at the late poststroke period. Semiquantitative analysis for the number of $CD4^+$T or $GITR^+$ cells in the ischemic region is shown in Figure 2g.

Predominant accumulation of $CD4^+GITR^+$T cells at the ischemic cortex after stroke. To confirm the enhanced expression of GITR on $CD4^+$T cells, we assessed the subset of T cells by FACS analysis using the cells extracted from the ischemic cortex[18] (Figures 3a and b). Consistent with the previous report, the brain extract contained substantial amount of mononuclear cells (Figure 3b) and FACS analysis detected a distinct subset of lymphocytes that had infiltrated the ischemic cortex (Figures 3c–f). We detected about 20% $CD4^+$T cells extracted from the infarcted brain tissue. We at first gated $CD3^+$ cells and then analyzed CD25 to characterize the corresponding

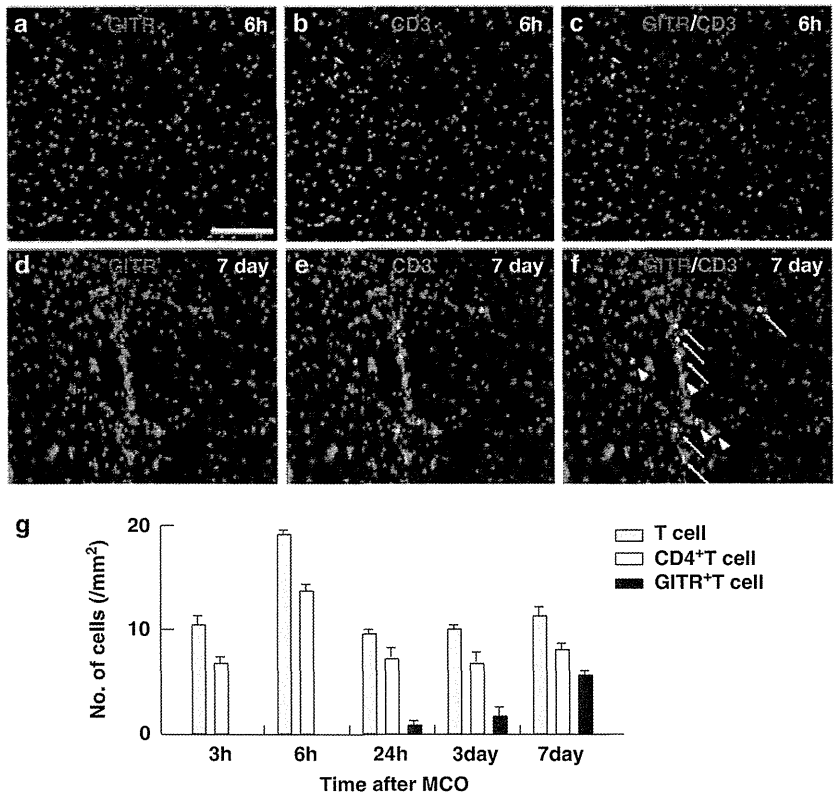

Figure 2 GITR-positive T-cell infiltration into the ischemic area of the poststroke brain. Immunohistochemistry for GITR$^+$T (**a–f**) cells infiltrated into the postischemic cortex 6 h (**a–c**) and 7 days (**d–f**) after stroke. The T cells were negative for GITR at 6 h (**a**: GITR; **b**: CD3; **c**: merged), but appeared to be positive for GITR at 7 days (arrows, **d**: GITR; **e**: CD3; **f**: merged). Arrowheads indicate GITR$^-$ T cells (**f**). (**a**) Scale bar: 100 μm. (**g**) Cells expressing CD3 (gray bars), CD4 (white bars) or GITR (black bars) 3 h, 6 h, 24 h, 3 days or 7 days after stroke were quantified. Results displayed are representative of three repetitions of the experimental protocol

CD4$^+$T cells. GITR was analyzed on CD3$^+$CD4$^+$ cells. No significant upregulation of CD25 on T cells was observed at days 1 and 7 after stroke (Figures 3c and e: 4.61% at day 1 and 4.06% at day 7). However, the percentage of GITR$^+$ T cells was increased from 6.17 to 86.50%, and the surface expression of GITR on CD4$^+$T cells at day 7 was significantly increased compared with that at day 1 (from 13.90 to 68.37 in mean channel value; Figures 3d and f), indicating enhanced expression of GITR as an activation marker for CD4$^+$T cells.

Effects of GITR triggering on cerebral infarction. Given that GITR triggering was involved in cerebral ischemic injury, we decided to examine whether stimulation or inhibition of GITR triggering affects cerebral infarction by using the same stroke model. Mice were treated with anti-GITR agonistic antibody (GITR–Ab: DTA-1), GITR–Fc fusion protein (blocking the GITR–GITRL interaction) or control IgG at 3 h and 3 days after stroke. The brain was then removed 30 days after stroke. The size of infarction in mice treated with GITR–Ab was apparently larger than that of mice treated with GITR–Fc (Figure 4a). Further analysis of the volume of each hemisphere based on brain sections demonstrated a significant decrease in the poststroke brain volume in GITR–Ab mice, and a significant increase in that of GITR–Fc mice, compared with control mice (Figure 4b). These findings indicated that ischemic injury was enhanced by GITR triggering, while ameliorated by its blocking.

Effects of GITR triggering on poststroke inflammation. We had until then attempted to determine how the triggering of GITR could affect poststroke inflammation. As several studies have reported that multiple cytokines modulate CNS inflammation,[2,3,19] the levels of IFN-γ, TNF-α and IL-10 were analyzed using quantitative real-time PCR in mice 7 days after stroke. The alteration of mRNA levels of these cytokines within the ischemic region was confirmed (Figure 4c–e). GITR–Ab treatment resulted in a significant elevation of IFN-γ ($P<0.05$) and TNF-α ($P<0.05$) levels, and a significant decrease in the IL-10 level ($P<0.01$) compared with the control IgG treatment. In contrast, treatment with GITR–Fc showed a significant decrease in IFN-γ ($P<0.01$) and TNF-α levels ($P<0.05$), and a significant increase in IL-10 level ($P<0.01$) compared with the control. These data indicated that GITR triggering largely affected cerebral ischemic injury by changing the level of poststroke inflammation (enhancing proinflammatory cytokines and suppressing anti-inflammatory cytokines).

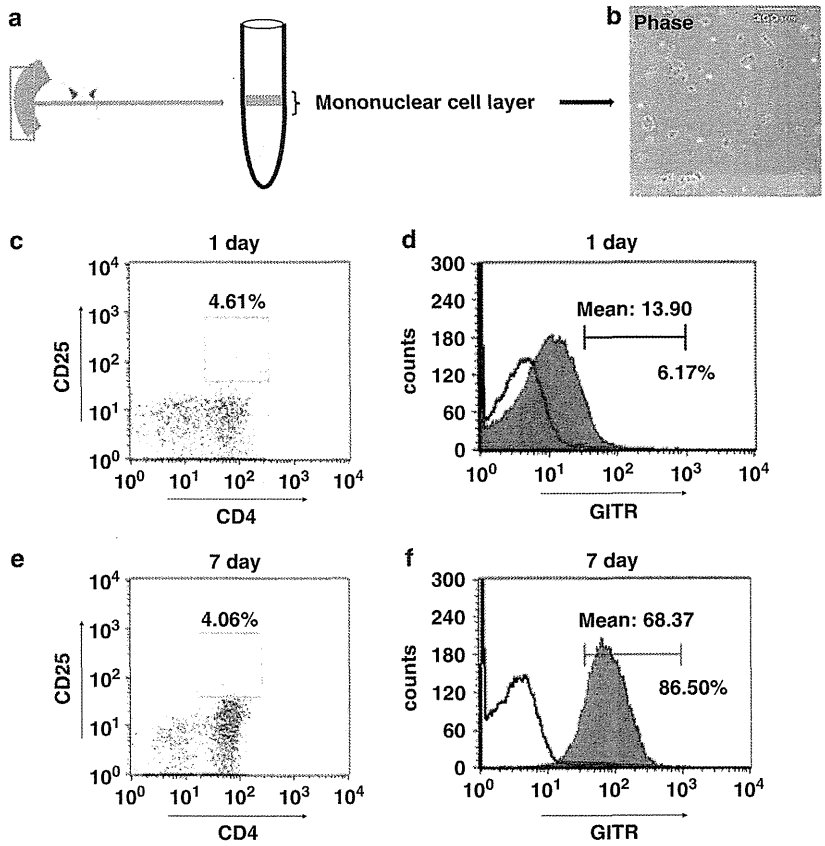

Figure 3 The analysis for the subpopulation of infiltrated cells in the ischemic area with FACS. (**a**) The ischemic tissue of the brain 7 days or 1 day after stroke was isolated and pressed through a cell strainer, and was separated by Ficoll-paque plus centrifugation. The extract contains lymphocyte-like mononuclear cells, which were observed under phase-contrast microscope. (**b**) FACS analysis for the subset of T cells that infiltrated the ischemic cortex was performed. The acquired lymphocytes were analyzed for $CD4^+$ and $CD25^+$ on $CD3^+$ cells 1 day (**c**) and 7 days (**e**), and for GITR on $CD3^+CD4^+$ cells 1 day (**d**) or 7 days (**f**) after stroke. The percentage of $CD25^+$ cells was evaluated in the total T cells ($CD3^+$ cells), and that of $GITR^+$ cells was evaluated in $CD4^+$ T ($CD3^+CD4^+$) cells extracted from the infarcted brain tissue. The mean channel values were displayed for GITR in the $CD3^+CD4^+$ cells. (**d** and **f**) Filled histogram represents GITR expression and open histogram represents isotype control

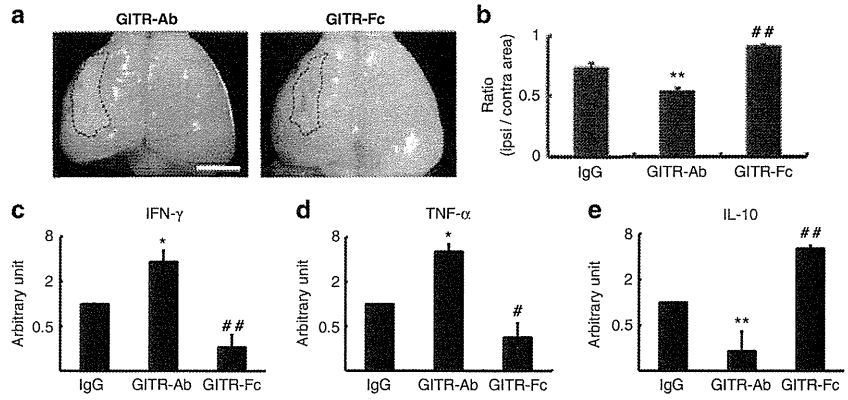

Figure 4 Effects of GITR triggering on the poststroke brain volume and cytokine expression. (**a**) On day 30 after stroke, brains of mice treated with either GITR–Ab or GITR–Fc were evaluated grossly. Areas of hatched line indicate infarct area. (**b**) Ipsilateral and contralateral cerebral hemisphere volume was calculated by integrating coronally oriented ipsilateral and contralateral cerebral hemisphere area. Involution of ipsilateral cerebral hemisphere volume calculated as (ipsilateral/contralateral cerebral hemisphere volume) confirmed a significant difference in brain volume in the poststroke hemisphere comparing the groups. (**b**) $n=5$ for each experimental group. (**a**) Scale bar: 2 mm. The expression of IFN-γ (**c**), TNF-α (**d**) and IL-10 (**e**) in the ischemic tissue on day 7 after stroke was detected by quantitative real-time PCR. The relative expression of mRNAs was represented as arbitrary unit, which was set at the level of the expression of the gene equal to 1 in the IgG-treated group using a logarithmic scale. The significance among the treatments was calculated from the relative level of mRNA expression. (**c–e**) $n=4$ for each experimental group. $^*P<0.05$ and $^{**}P<0.01$, GITR–Ab-treated mice *versus* control IgG-treated mice; $^{\#}P<0.05$ and $^{\#\#}P<0.01$, GITR–Fc-treated mice *versus* control IgG-treated mice

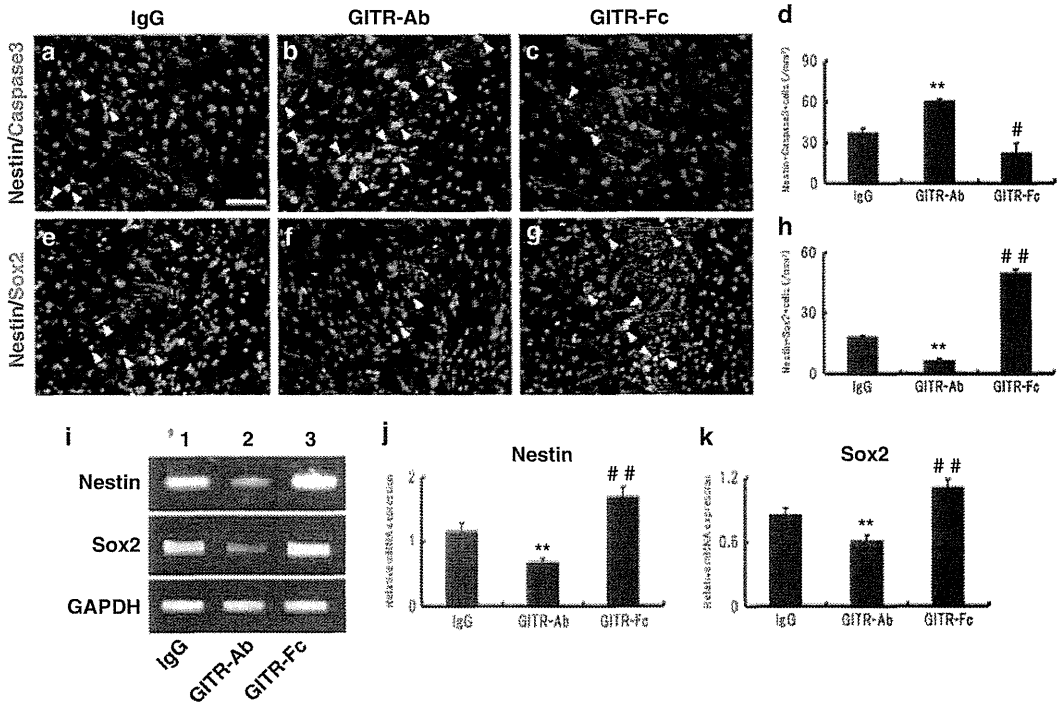

Figure 5 Effects of GITR–Ab or GITR–Fc on survival/death of neural stem/progenitor cells. (**a–d**) Co-expression of nestin (red) and active caspase-3 (green; arrowheads) was investigated 3 days after stroke at the border of the infarction. Compared with the control IgG-treated mice (**a**), GITR–Ab-treated mice showed an increased number of nestin/caspase-3-positive cells (**b**), whereas GITR–Fc-treated mice showed fewer co-expressing cells (**c**). (**e–h**) Co-expression of nestin (red) and Sox2 (green; arrowheads) was investigated 7 days after stroke. Few cells co-expressing nestin and Sox2 were observed in GITR–Ab-treated mice (**f**), whereas a number of nestin/Sox2-co-expressing cells were observed in GITR–Fc-treated mice (**g**). The number of nestin/caspase-3 cells (**d**) and nestin/Sox2 cells (**h**) at each period was significantly different on comparing the groups. (**d**) $n=3$ and (**h**) $n=4$ for each experimental group. (**i–k**) Expression of nestin or Sox2 was detected by conventional RT-PCR in the ischemic tissue on day 7 (**i**). Compared with the control IgG-treated mice (first lane), GITR-treated mice showed decreased expression of nestin or Sox2 (second lane), whereas GITR–Fc-treated mice showed increased expression (third lane). The relative expression was significantly different on comparing the groups (**j**: nestin; **k**: Sox2). (**j**) $n=4$ and (**k**) $n=5$ for each experimental group. (**a**) Scale bar: 100 μm. $^{**}P<0.01$, GITR–Ab-treated mice *versus* control IgG-treated mice; $^{\#}P<0.05$ and $^{\#\#}P<0.01$, GITR–Fc-treated mice *versus* control IgG-treated mice

Effects of GITR triggering on survival/death of neural stem/progenitor cells. Inflammation is known not only as a deteriorated factor of cerebral injury but also as a strong stimulator of neurogenesis. As the current study has proved that GITR triggering can regulate the inflammatory response,[15,17] we assessed the GITR–GITRL interaction, which may contribute to neurogenesis in the infarction area. Because we had previously showed that iNSPCs could contribute to poststroke neurogenesis and that cortical neurogenesis is related to the development of the iNSPCs,[8,20,21] the effects of GITR–Ab or GITR–Fc on survival/death of iNSPCs were investigated by using immunohistochemistry for nestin and active caspase-3 on the ischemic brain sections. The nestin-positive iNSPCs were observed at the border of the infarction as well as in the ischemic core 7 days after stroke (see Supplementary Figure 1B, red, nestin) as described.[6,8,20] Control IgG-treated mice appeared to have abundant nestin and active caspase-3 double-positive cells (Figure 5a, red, nestin; green, caspase-3). The administration of GITR–Ab increased the number of nestin/caspase-3 cells (Figure 5b), whereas that of GITR–Fc decreased it (Figure 5c). The number of activated caspase-3-positive iNSPCs was significantly different among the three groups (Figure 5d; $^{**}P<0.01$, GITR–Ab *versus* control IgG; $^{\#}P<0.05$, GITR–Fc *versus* control IgG). These findings indicate that GITR triggering induced, whereas its blocking suppressed, apoptosis of iNSPCs.

To provide further support for our hypothesis that GITR triggering participates in iNSPC-death/survival, expressions of nestin and Sox2 (SRY (sex determining region Y)-box 2), neural stem cells markers,[22] were assessed by immunohistochemistry (Figures 5e–h). Seven days after stroke, a number of nestin-positive cells express Sox2, especially at the border of infarction (Supplementary Figures 1A–D). The administration of GITR–Ab significantly decreased the number of nestin/Sox2 double-positive cells (Figures 5f and h; $P<0.01$ *versus* control IgG), whereas the administration of GITR–Fc increased them (Figures 5g and h; $P<0.01$ *versus* control IgG). These findings were confirmed by conventional reverse transcription (RT)-PCR (Figures 5i–k) using mRNA extracted from the infarcted cortex (Figure 5i). Relative expressions of nestin and Sox2 were attenuated by GITR–Ab treatment, and enhanced by GITR–Fc treatment (Figures 5j and k; $P<0.01$, among the three groups).

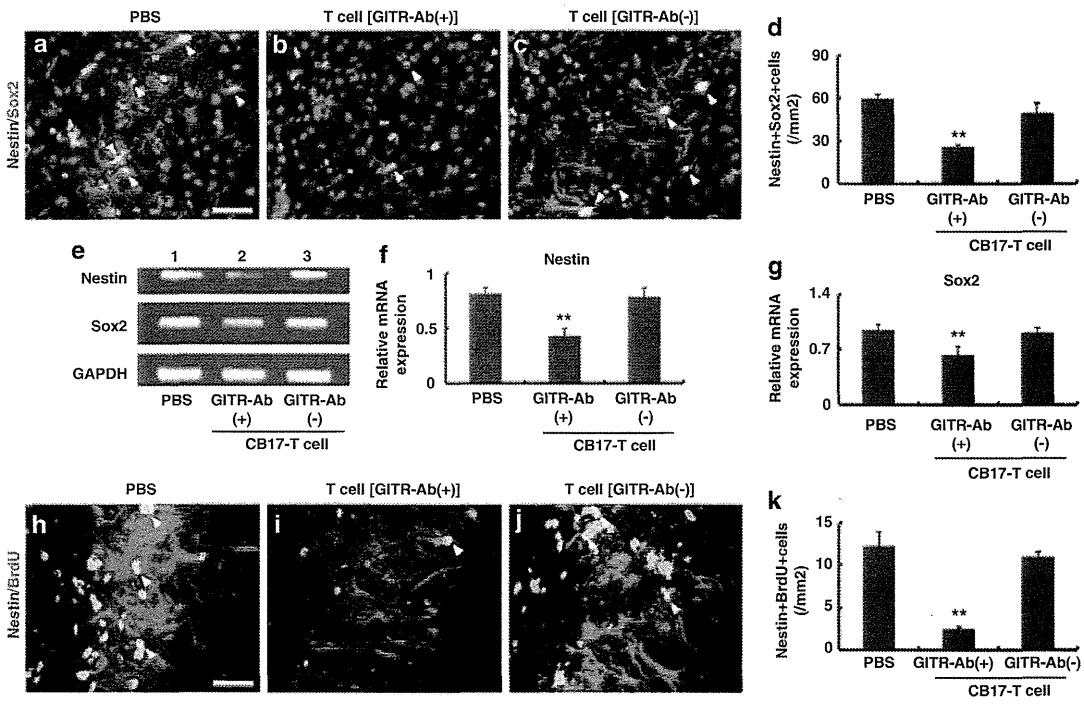

Figure 6 Effects of administration of T cells triggered by GITR on survival/death of neural stem/progenitor cells. (**a–d**) Co-expression of nestin (red) and Sox2 (green; arrowheads) was investigated 7 days after stroke in SCID mice, which were injected with T cells. Compared with the PBS-injected control mice (**a**), mice treated with GITR-stimulated T cells showed significantly less nestin/Sox2-positive cells (**b**), whereas mice treated with non-stimulated (control-IgG stimulated) T cells showed no difference compared with the control (**c**). (**d**) $n=6$, 3 and 3 for PBS-, GITR-stimulated T cell and non-stimulated T cell-treated groups, respectively. Expression of nestin or Sox2 detected by conventional RT-PCR in the ischemic tissue on day 7 (**e**) was significantly decreased after treatment with GITR-stimulated T cells (**e**: second lane) compared with control (PBS; **e**: first lane) or non-stimulated T-cell treatment (**e**: third lane; **f**: nestin; **g**: Sox2). (**f** and **g**) $n=5$ for each experimental group. (**h–k**) The number of proliferated neural stem/progenitor cells evaluated with anti-nestin (red) and anti-BrdU (green) antibodies (arrowheads) on day 7 was significantly decreased after treatment with GITR-stimulated T cells (**i**), compared with control (**h**) or non-stimulated T cell-treatment (**j**). Quantitative analysis confirmed the decreased number of nestin/BrdU-positive cells in GITR-stimulated T-cell-treated mice, compared with the other two groups (**k**; $n=5$ for each experimental group). $^{**}P<0.01$ *versus* PBS- or non-stimulated T cell-treated (GITR–Ab(−)/CB-17 T cell) mice. (**a** and **h**) Scale bar: 50 μm

Effects of GITR-stimulated T cells on survival/death of neural stem/progenitor cells. As the ischemic insult enhanced the expression of GITR on infiltrated $CD4^+$ T cells (Figures 1–3) and GITR triggering disrupted iNSPCs in poststroke mice (Figure 5), we next investigated whether GITR-triggered, activated $CD4^+$T cells could affect survival/death of iNSPCs. Activation of $CD4^+$T cells by ligation of GITR has been reported previously,[17] and we also confirmed enhanced expression of GITR on $CD4^+$T cells by GITR–Ab (DTA-1; see Figure 8d; lanes 3, 4). Initially, to confirm infiltration of the administered T cells into the ischemic area, T cells extracted from the green fluorescence protein-transgenic (GFP-Tg) mice were injected into SCID mice 2 days after stroke as described previously.[7,20] Five days after administering, the GFP-positive T cells migrated selectively into the infarction area of the poststroke brain (Supplementary Figure 2). Next, we injected T cells of CB-17 mice (either stimulated or non-stimulated by GITR–Ab) as described above, and examined the expressions of nestin/Sox2 double-labeled cells 5 days after injection by immunohistochemistry (Figures 6a–d). In accordance with our previous report,[8] poststroke SCID mice with PBS injection (control) expressed a greater number of nestin/Sox2-positive iNSPCs than CB-17 mice (compare Figure 6d with Figure 5h). The administration of GITR-stimulated T cells significantly decreased the number of nestin/Sox2 cells (Figures 6b and d; $P<0.01$), whereas non-stimulated T cells had no significant effect (Figures 6c and d). These findings were confirmed by conventional RT-PCR analysis (Figure 6e). Relative expressions of both nestin and Sox2 were attenuated by administration of GITR-stimulated T cells but not by non-stimulated T cells (Figures 6f and g). The proliferation of iNSPCs was also evaluated by labeling of nestin-positive cells with bromodeoxyuridine (BrdU), as per a previous report.[8] GITR-stimulated T cells significantly decreased the number of BrdU-labeled nestin-positive cells compared with PBS treatment as a control (Figures 6i and k; $P<0.01$), whereas non-stimulated T cells had no significant effect (Figures 6j and k). These findings indicate that GITR-triggered, activated $CD4^+$T cells, but not non-stimulated T cells, affect survival/death of iNSPCs after stroke.

***In vitro* effects of TNF-α and Fas ligand on apoptosis of neural stem/progenitor cells.** To determine how activated $CD4^+$T cells ligated by GITR affect survival/death of iNSPCs, a cell death assay was performed using cultured neurospheres consisting of iNSPCs (Figure 7a). It is well known that some neural stem/progenitor cells undergo

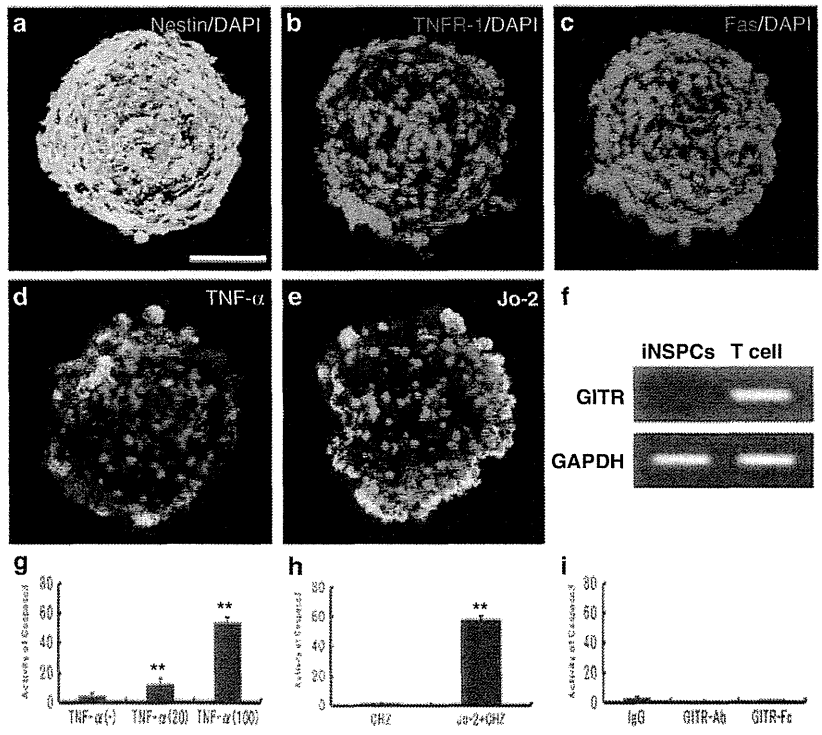

Figure 7 Involvement of death factors in apoptosis of iNSPCs neurospheres. In neurospheres obtained from the ischemic areas of poststroke mice, nestin (green; **a**), TNFR-1 (red; **b**) and Fas (red; **c**) were virtually observed (DAPI, blue). Incubation with TNF-α (**d**) or Jo-2 (**e**) induced collapse of cell clusters with expression of a marker of apoptotic cell death, anionic phosphatidylserine visualized with Annexin V staining (green). (**f**) GITR was not expressed on iNSPCs neurosphere. (**g**) Incubation with TNF-α increased the activity of caspase-3 in neurospheres in a dose-dependent manner. Jo-2 also increased the activity (**h**), but neither GITR–Ab (DTA-1) nor GITR–Fc activated caspase-3 on the neurospheres (**i**). (**a** and **d**) Scale bar: 100 μm. (**g**–**i**) $n=3$ for each experimental group. $^{**}P<0.01$ *versus* control groups (**g**: without TNF-α; **h**: CHZ without Jo-2). No significant difference was found among the groups (**i**)

apoptosis, with expression of multiple cell death signals such as TNF receptor-1 (TNFR-1)[23] and Fas.[8] Consistent with these studies, we confirmed expression of TNFR-1 (Figure 7b) and Fas (Figure 7c) on iNSPC neurospheres. The neurospheres were incubated with Dulbecco's modified Eagle's medium (DMEM) containing TNF-α or agonistic Fas antibody (Jo-2) for 24 h, and their apoptosis was analyzed by Annexin V staining and active caspase-3 assay. As expected, TNF-α induced apoptosis of neurosphere cells (Figure 7d; green: Annexin V, red: PE). The activity of caspase-3 in the apoptotic neurosphere was increased dose dependently by TNF-α (Figure 7g). Jo-2 also induced apoptosis of neurospheres (Figure 7e), with a significant increase in caspase-3 activity (Figure 7h). Because iNSPCs neurosphere do not express GITR (Figure 7f), it is not likely that GITR signaling regulates death-receptor-induced apoptosis directly in iNSPCs. Accordingly, neither GITR–Ab nor GITR–Fc activated caspase-3 on the neurospheres (Figure 7i). These findings suggest that the death signaling pathway may be stimulated either directly or indirectly by activated $CD4^+$T cells ligated by GITR. Moreover, these results also prove that the triggering of GITR directly have no effect on apoptosis of iNSPCs.

Effect of GITR-stimulated Gld-T cells on survival/death of neural stem/progenitor cells. To assess the action of activated T cells, neurospheres were incubated with T cells (either GITR stimulated or non-stimulated) for 24 h (Figures 8a and b). Consistent with previous studies,[16,24] T cells stimulated by GITR–Ab showed upregulation of Fas ligand (FasL) expression (Figures 8c and d; lanes 3 and 4) as well as GITR expression (Figure 8d; lanes 3 and 4). Annexin V staining showed that neurospheres coincubated with GITR-stimulated T cells underwent apoptosis (Figure 8a), but those with non-stimulated T cells did not (Figure 8b). This result strongly suggested a role of FasL expressed on T cells in the iNSPCs apoptosis. Because nestin-positive iNSPCs were frequently observed in close association with endothelial cells[20,21] and $CD4^+$T cells (Supplementary Figure 3) in the poststroke brain, it is highly possible that activated T cells induce apoptosis of iNSPCs by cell to cell interactions.

To confirm this hypothesis *in vivo*, we administered T cells from the FasL-deficient (generalized lymphoproliferative disorder = spontaneous mutation in the Fas ligand gene; gld) mice,[25] stimulated by GITR–Ab, to poststroke SCID mice and analyzed the expression of nestin and Sox2 in the postischemic area by conventional RT-PCR. As gld-T cells stimulated by GITR–Ab showed enhanced GITR expression compared with non-stimulated gld-T cells similar to T cells from wild-type mice (Figure 8d; lanes 1 and 2, Figure 8f), the injected T cells were considered to be activated without

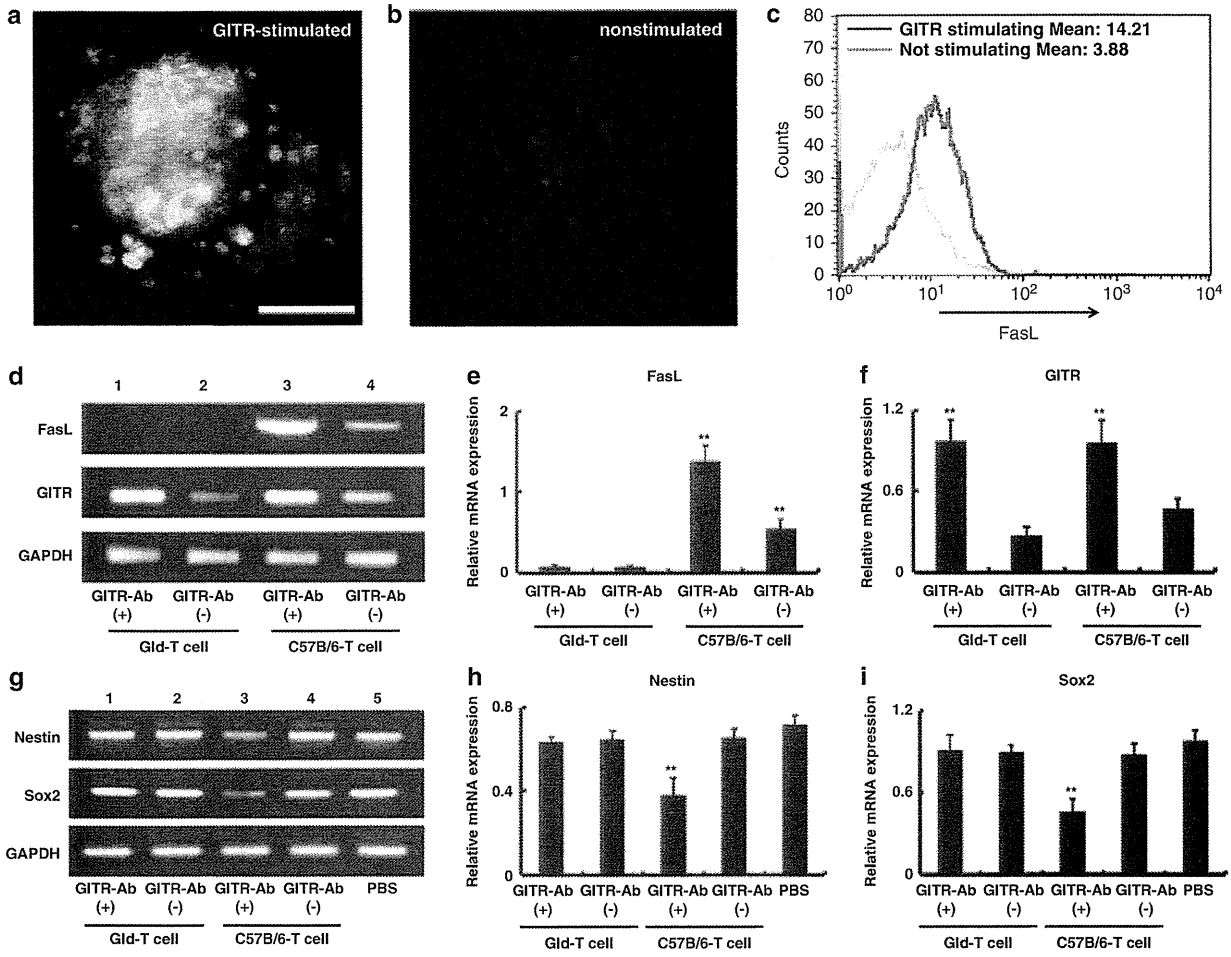

Figure 8 Involvement of Fas ligand expressed on the surface of T cells in survival/death of neural stem/progenitor cells. Incubation with GITR-stimulated T cells induced apoptotic cell death on neurospheres determined by Annexin V staining (**a**: green), whereas no cell death was observed in the presence of non-stimulated T cells (**b**). The upregulated FasL expressed on GITR-stimulated T cells was confirmed by FACS analysis (**c**: red line indicates the FasL expression on GITR-stimulated T cells, and green line on non-stimulated T cells in $CD4^+$ T cells). The mean channel values were displayed for FasL in the $CD4^+$ T cells. Conventional RT-PCR showed that T cells obtained from Gld mice (Gld-T cell) never expressed Fas ligand even after GITR stimulation (**d**: lanes 1 and 2; **e**), whereas T cells of wild C57/B6 mice expressed it (**d**: lanes 3 and 4; **e**). GITR stimulation upregulated GITR on T cells regardless of the presence of FasL (**d**: lanes 1 and 3; **f**). The group of GITR-stimulated T cells from C57B/6 only significantly upregulated FasL (**d** and **e**). (**a**) Scale bar: 100 μm. (**e** and **f**) $n=5$ for each experimental group. $^{**}P<0.01$ *versus* Gld-T cell groups or non-stimulated T (GITR–Ab(−)/C57B/6-T) cell group. Expression of nestin or Sox2 detected by conventional RT-PCR in the ischemic cortex of SCID mice 7 days after stroke was not affected by administration of Gld-T cells stimulated by GITR–Ab (**g**: first *versus* second lanes; **h** and **i**), although it was significantly decreased after treatment with wild-type (C57B/6) T cells stimulated by GITR-Ab (**g**: third *versus* fourth lanes; **h** and **i**). The relative expression of nestin or Sox2 was significantly suppressed only in the case of mice administered with FasL-expressed T cells stimulated by GITR–Ab. (**h** and **i**) $n=5$ for each experimental group. $^{**}P<0.01$ *versus* Gld-T cell groups, GITR(−)/C57B/6-T-cell group or PBS group. No significant difference was found among the other groups

expression of FasL (Figure 8e). Although administration of GITR-stimulated T cells from wild mice (C57/B6) significantly attenuated nestin and Sox2 expression (Figure 8g; lanes 3 and 4), administration of GITR-stimulated gld-T cells had no significant effect (Figure 8g; lanes 1 and 2). Relative expressions of nestin and Sox2 were attenuated only by GITR-stimulated wild-type T cells from wild mice, but not by GITR-stimulated gld-T cells or non-stimulated T cells (Figures 8h and i; $P<0.01$, among the five groups). These findings indicate that GITR-triggered activated $CD4^+$T cells directly induce Fas-mediated apoptosis of iNSPCs through possible cell to cell interactions.

Discussion

This study clearly demonstrated a key role of GITR triggering in regulation of neurogenesis after stroke, thereby delineating the contribution of activated T cells expressing GITR to the survival of neural stem/progenitor cells in the poststroke cortex. Because a subset of $CD4^+$T cells mainly expresses GITR after stroke, it is likely that activated $CD4^+$T cells triggered by GITR are harmful to the new-born cells. The current study also suggests possible mechanisms involving FasL- and TNF-α-induced cell death signals, suggesting interactions between iNSPCs and GITR-triggered T cells,

with the latter serving as negative regulators for CNS repair after cerebral infarction.

GITR was originally cloned from a glucocorticoid-treated hybridoma T-cell line as a TNF-receptor-like molecule induced by glucocorticoid-sensitive T cells.[12] GITR is now considered to be upregulated in T cells by T-cell receptor (TCR)-mediated activation.[26] As GITR-expressing T cells are resistant to glucocorticoid-induced cell death, it has been proposed that GITR, in conjunction with other TCR-induced factors, protects T cells from apoptosis.[26] In fact, GITR can be upregulated by viral infection[27] or acute lung inflammation.[15] In the present study, we have demonstrated for the first time that GITR is upregulated in T cells by ischemic insult to the brain, although previous reports have shown the role of GITR in ischemic damage on the kidney or the intestine.[28,29]

Consistent with our previous study,[8] $CD4^+$T cells predominantly migrated to the infarcted brain after stroke. The high number of $GITR^+CD4^+$T cells suggested that activated T-cell proliferation contributed to the poststroke inflammatory response. GITR has been reported to enhance the secretion of proinflammatory cytokines, such as IL-2 and IFN-γ, from $GITR^+$T cells.[30] In contrast, GITR triggering on $CD4^+CD25^+$Treg completely abrogates the suppressing effect of Treg,[13] which normally secrete anti-inflammatory cytokines such as IL-10.[31] Thus, we suggest that upregulation of the GITR expression in the brain can aggravate T-cell-mediated poststroke inflammation. The present study demonstrated that GITR triggering in poststroke mice enhanced, and its blocking ameliorated the poststroke inflammatory response as indicated by modulation of cytokines, such as IFN-γ, TNF-α and IL-10. These data suggest that T-cell-mediated poststroke inflammation can be modulated by the immune response deriving from GITR–GITRL interaction.

It is well known that cerebral injury induces a disturbance of the normally well-balanced interplay between the immune system and the CNS.[32] This process results in homeostatic signals being sent to various sites in the body through pathways of neuroimmunomodulation, including hypothalamic–pituitary–adrenal (HPA) axis. Activation of the HPA axis results in the production of glucocorticoid hormones. Although glucocorticoid does prevent inflammation by suppressing production of many proinflammatory mediators, including cytokines such as IL-1β and TNF-α, it also induces apoptosis in immature and mature T lymphocytes.[33] The latter may in turn lead to secondary immunodeficiency.[32] Alternatively, surviving T cells that are resistant to glucocorticoid stress express GITR and may contribute to the aggravation of inflammation.

Inflammation in neural tissue has long been suspected to have a role in stroke. Immune influence on adult neural stem cell regulation and function has also received much attention. Although the details of immune signaling in the CNS are not known, the impact of inflammatory signaling on adult neurogenesis is known to be focused on the activation of microglia as a source of proinflammatory cytokines, such as TNF-α, IL-6 and IL-1β. We and others[34] have proved that neural stem cells undergo apoptosis by TNF-α *in vitro*, suggesting that TNF-α has a negative effect on poststroke neurogenesis. Recent publication has revealed that GITR and GITRL are functionally expressed on brain microglia, and that the stimulation of GITRL can induce inflammatory activation of microglia.[35] However, as iNSPCs never expressed GITR, it is more likely that microglia contribute to iNSPC cell death indirectly via TNF-α, which is secreted from the activated microglia. We also propose that IFN-γ produced by activated $GITR^+$T cells stimulates microglia production of high levels of TNF-α to induce apoptosis of iNSPCs through TNFR-1. It also has been reported that TNF-related apoptosis-inducing ligand (TRAIL) has an important role in developing CNS injury, and that anti-TRAIL treatment prevents GITR expression induced by spinal cord injury.[36] As GITR-deficient mice showed attenuated TRAIL expression after SCI, blocking the GITR–GITRL interaction by GITR–Fc protein may protect from the inflammatory response via TRAIL-activated pathways.

In addition to cytokine effects on neurogenesis, we also proposed the Fas-mediated pathway that affects poststroke neurogenesis, as another target of immune signaling. Our previous study[8] had shown that Fas-positive iNSPCs underwent apoptosis in the poststroke cortex. The current study confirmed that $GITR^+$T cells expressing FasL triggered apoptosis of iNSPC *in vitro* and reduced the expression of nestin and Sox2 in the poststroke brain. These findings suggest that activated T cells act on Fas-expressing iNSPCs via cell to cell interactions in the poststroke brain, although it is very difficult to prove the functional contact between iNSPCs and Fas-expressing T cells *in vivo*. As nestin-positive iNSPCs are in close association with endothelial cells[20,21] where $CD4^+$T cells are infiltrated (Supplementary Figure 3), it is possible that activated T cells are in contact with neural stem/progenitor cells when the endothelial cells are damaged by ischemic insult. Although another system that activates neurogenesis through soluble FasL and Fas receptor in conventional neurogenic regions has been previously reported,[37] the current study may prove that the membrane-bound FasL expressed on T cells is essential for Fas-induced apoptosis.[38]

Recent study has proposed the contribution of Tregs in prevention of secondary infarct growth.[2,4] Because IL-10 signaling was mainly produced by $CD4^+CD25^+$Tregs and proinflammatory cytokines were downregulated in brains of IL-10 transgenic mice, Tregs apparently contribute to the anti-inflammatory system after stroke. Although $GITR^+$T cells are known to belong to Tregs, a recent study has emphasized that GITR is a marker for activated effector T cells.[39] The $CD4^+CD25^-$ T-cell-derived $GITR^+$ cells ($GITR^+$ non-Treg) are also known to activate self-reactive T cells by attenuating the function of Tregs,[13] indicating that they may harm the living cells by eliciting autoimmunity.[13,24] We demonstrated in the current study that blocking the GITR–GITRL interaction by GITR–Fc protein increased IL-10 expression in the poststroke cortex, suggesting that blocking such interactions enhanced Treg function as well as inhibition of effector T cell function. On the basis of these findings, the present study suggests that the novel therapies for stroke may ultimately include GITR-targeted manipulation of immune signaling.

Materials and Methods

All procedures were carried out under auspices of the Animal Care Committee of Hyogo College of Medicine, and were in accordance with the criteria outlined in the 'Guide for the Care and Use of Laboratory Animals' prepared by the National

Academy of Science. Quantitative analyses were conducted by investigators who were blinded to the experimental protocol and identity of the samples under study.

Induction of focal cerebral ischemia. Male, 5- to 7-week-old, CB17/Icr $^{+/+}$ Jcl mice (CB-17 mice; Clea Japan Inc., Tokyo, Japan) and CB-17/Icr$^{scid/scid}$ Jcl mice (SCID mice; CLEA Japan Inc.) were subjected to cerebral ischemia. Permanent focal cerebral ischemia was produced by ligation and disconnection of the distal portion of the left middle cerebral artery (MCA), as described in a previous study. In brief, the left MCA was isolated, electrocauterized and disconnected just distal to its crossing of the olfactory tract (distal M1 portion) under halothane inhalation. The infarcted area in mice of this background has been shown to be highly reproducible and limited to the ipsilateral cerebral cortex. Permanent MCA occlusion (MCO) is achieved by coagulating the vessel. In sham-operated mice, arteries were visualized but not coagulated.

Immunohistochemistry. To histochemically analyze the infarcted cortex, mice were deeply anesthetized with sodium pentobarbital and perfused transcardially with 4% paraformaldehyde. Brains were then removed, and coronal sections (14 μm) were stained with mouse antibodies against nestin (Millipore, Billerica, MA, USA; 1/100), Sox2 (Millipore; 1/100), NeuN (Millipore; 1/200), rabbit antibodies against caspase-3 active (R&D systems, Minneapolis, MN, USA; 1/100), CD3 (AnaSpec, San Jose, CA, USA; 1/100), CD31 (Santa Cruz Biotechnology, Santa Cruz, CA, USA; 1/100), rat antibody against CD4 (Biolegend, San Diego, CA, USA; 1/100) and GITR (eBioscience, San Diego, CA, USA; 1/100). As secondary antibodies, Alexa Fluor 488 or Alexa Fluor 555 goat anti-mouse, -rabbit or -rat IgG (Invitrogen, Carlsbad, CA, USA; 1/500) was used. Cell nuclei were stained with 4′, 6-diamino-2-phenylindole (DAPI, Kirkegaard & Perry Laboratories, Gaithersburg, MD, USA; 1/500). The number of nestin and Sox2 double-positive cells at the border of infarctions, including the infarcted and peri-infarcted areas (0.5 mm in width), was counted under a laser microscope (Olympus Corporation, Tokyo, Japan).

To perform quantitative analysis of T cells, all CD3–, CD4– or CD3–GITR-double-positive cells within the infarcted area were counted in the brain sections obtained from CB-17 mice at 3 h, 6 h, 24 h, 3 days and 7 days after stroke. Furthermore, active caspase-3 and nestin double-positive cells within the infarcted area were counted in the brain sections at 3 days after stroke. To investigate cell proliferation at 7 days after stroke, BrdU (Sigma-Aldrich Corporation, St. Louis, MO, USA; 50 mg/kg) was administered 6 h before fixation. Tissue was pretreated with 2N HCl for 30 min at 37°C and 0.1 M boric acid (pH 8.5) for 10 min at room temperature, and then stained with antibody against BrdU. Next, the number of positive cells for each marker was determined using modified Image J (National Institute of Mental Health, Bethesda, MD, USA) as per a previous report.[8] Results were expressed as the number of cells/mm^2.

The expression of Fas and TNFR-1 for neurosphere. To study the expression of Fas and TNFR-1in the neurosphere *in vitro*, immunochemistry was performed with rabbit antibody against Fas (Wako Pure Chemical Industries, Osaka, Japan; 1/100) or TNFR-1 (Santa Cruz Biotechnology; 1/100). As secondary antibodies, Alexa Fluor 488 or Alexa Fluor 555 goat anti-mouse IgG (Invitrogen; 1/500) was used. Cell nuclei were stained with DAPI (Kirkegaard & Perry Laboratories; 1/500).

Measurement of involution of the ipsilateral cerebral hemisphere volume. Thirty days after stroke, mice were perfused transcardially with 4% paraformaldehyde, brains were removed and coronal sections (14 μm) were stained with mouse antibodies against NeuN, followed by reaction with biotinylated goat anti-mouse IgG (Chemicon, Temecula, CA, USA; 1/500), ABC Elite reagent (Vector Laboratories, Burlingame, CA, USA) and DAB (Sigma-Aldrich Corporation) as chromogen. The area of the ipsilateral and contralateral cerebral hemisphere occupied by the neuronal markers, NeuN and MAP2, was calculated using Image J.[8] The ipsilateral and contralateral cerebral hemisphere volume was calculated by integrating the coronally oriented ipsilateral and contralateral cerebral hemisphere area as described previously.[8] Involution of the ipsilateral cerebral hemisphere volume was calculated as (ipsilateral/contralateral cerebral hemisphere volume).

FACS analysis of infiltrated lymphocytes into the ischemic brain. Animals were killed 1 or 7 days after MCO. The ischemic area of the brain was isolated. Tissues from the four operated mice were incubated with RPMI1640 (Invitrogen), containing 1 mg/ml collagenase (Wako Pure Chemical Industries) and 0.1 mg/ml DNAse I (Thermo Fisher Scientific, Waltham, MA, USA), and pressed through a 40-μm cell strainer[18] (BD Biosciences, Franklin Lakes, NJ, USA). The mononuclear cells were separated by Ficoll-paque plus (GE Healthcare, Piscataway, NJ, USA) centrifugation, and labeled with antibody cocktails (Per CP-CD3 (BD Biosciences), FITC-CD4 (eBioscience), PE-GITR (BD Biosciences) and APC-CD25 (eBioscience)). Rat IgG2a (eBioscience) was used as control isotype staining. The analysis of cells was performed by four-color flow cytometry on a FACSCalibur (BD Biosciences) using CELLQuest Software (BD Biosciences).

RNA isolation and PCR reaction. Total RNA was isolated from the cerebral cortex of the infarcted area using ISOGEN (Nippon gene, Tokyo, Japan), and was treated using Turbo DNA-free kit (Applied Biosystems, Foster city, CA, USA) in accordance with the manufacturer's protocol.

Quantity and quality of the isolated RNA was tested by using a Nanodrop 1000 (Thermo Fisher Scientific).

Quantitative real-time PCR was performed using TaqMan Gene Expression Assays and the ABI PRISM 7900HT Sequence Detection System (Applied Biosystems) with Real-time PCR Master Mix (Toyobo, Osaka, Japan). Three replicates were run for each sample in a 384-well format plate. TaqMan Gene Expression Assays IDs were described as follows. IFN-γ: Mm01168134_m1, TNF-γ: Mm00443258_m1, IL-10: Mm01288386_m1 and glyceraldehyde-3-phosphate dehydrogenase (GAPDH): Mm99999915_g1.

Conventional RT-PCR was performed using a PC-708 (Astec, Fukuoka, Japan) with Super Script III One step (Invitrogen). cDNA was amplified under the following conditions: 15 s at 94°C, 30 s at 60°C and 1 min at 68°C (35 cycles). PCR products were analyzed by electrophoresis using Mupid (Advance, Tokyo, Japan). The band intensity was determined with a LAS-1000 densitometer (Fuji Film, Tokyo, Japan). Primer sequences were as follows:

nestin, forward 5′-CACTAGAAAGCAGGAACCAG-3′ and reverse 5′-AGATGG TTCACAATCCTCTG-3′;
Sox2, forward 5′-TTGGGAGGGGTGCAAAAAGA-3′ and reverse 5′-CCTGCGA AGCGCCTAACGTA-3′;
GITR, forward 5′-CCACTGCCCACTGAGCAATAC-3′ and reverse 5′-GTAAAAC TGCGGTAAGTGAGGG-3′;
FasL, forward 5′-CTTGGGCTCCTCCAGGGTCAGT-3′ and reverse 5′-TCTCCT CCATTAGCACCAGATCC-3′; and
GAPDH, forward 5′-GGAAACCCAGAGGCATTGAC-3′ and reverse 5′-TCAGG ATCTGGCCCTTGAAC-3′.

For normalization of real-time data, GAPDH was used as an internal control.

Preparation of induced neural stem/progenitor cells. As described previously,[6] tissue from the ischemic cortex was mechanically dissociated by passage through 23- and 27-gauge needles to prepare a single-cell suspension. The resulting cell suspensions were incubated in a medium promoting formation of neurosphere-like clusters. Cells were incubated in tissue culture dishes (60 mm) with DMEM/F12 (Invitrogen) containing epidermal growth factor (EGF; Peprotech, Rocky Hill, NJ, USA; 20 ng/ml) and fibroblast growth factor-basic (FGF-2; Peprotech; 20 ng/ml). On day 7 after incubation, neurosphere-like cell clusters (primary spheres) were formed and were reseeded at a density of 10–15 neurospheres/well in 12-well low-binding plates.

Induction of apoptosis of neural stem/progenitor cells. To study the effect of TNF-α- or Fas-mediated signaling *in vitro*, neurospheres were incubated with TNF-α (R&D systems; 20 mg/ml and 100 mg/ml) or agonistic anti-Fas (Jo-2; BD Biosciences; 1 μg/ml) containing cycloheximide (CHZ; Sigma-Aldrich Corporation; 1 mg/ml),[40] agonistic anti-GITR (DTA-1; 10 μg/ml) or GITR–Fc fusion protein (6.25 μg/ml, Alexis Corporation, Lausen, Switzerland) in DMEM/F12 (Invitrogen) for 24 h. Next, the activity of caspase-3 was examined using a caspase-3 assay kit (Sigma-Aldrich Corporation) according to the manufacturer's protocol. Briefly, neurospheres were homogenized in lysis buffer and centrifuged at 20 000 *g* for 15 min. Supernatants were mixed with assay buffer and caspase-3 substrate. Absorbance at 405 nm was measured, and caspase-3 activity was calculated ($n = 3$, in each group) using a spectrophotometer (Beckman Coulter Inc., Brea, CA, USA). Caspase-3 activity was correlated with the protein concentration, which was determined by the DC protein assay (Lowry method; Bio-rad Laboratories Inc., Hercules, CA, USA). To confirm the cells undergoing apoptosis, neurospheres incubated with these reagents were stained with Annexin V (BD Biosciences), and were observed under a confocal laser scanning microscope (Carl Zeiss International, Jena, Germany).

To examine the apoptotic activity of T cells *in vitro*, T cells were obtained from the spleens of mice (several strains) involving CB-17 and gld (FasL deficient) and their C57/B6 backgrounds,[25] by using a nylon fiber column (Wako Pure Chemical Industries). T cells also were obtained from normal male C57BL/6 (Japan SLC, Shizuoka, Japan) or C57BL/6-Tg (CAG-EGFP) C14-Y01-FM131Osb transgenic mice (purchased from RIKEN BRC, Tsukuba, Japan). The T cells were stimulated with solid phase of anti-CD3ε antibody (BD Bioscience): T cells were incubated with GITR–Ab (DTA-1: 10 μg/ml) or control rat IgG (eBioscience) for 48 h in RPMI1640 (Invitrogen) in culture plate coated with 10 μg/ml of anti-CD3e antibody. Expression of FasL on GITR-stimulated T cells or non-stimulated T cells was analyzed with FACS. Each sample was labeled with antibody cocktails (PerCP-CD3, FITC-CD4 and PE-FasL (BD Biosciences)) The analysis of cells was performed by three-color flow cytometry on a FACSCalibur using CELLQuest Software. Then, 1×10^6 T cells were coincubated with neurospheres in DMEM/F12 (Invitrogen) for 24 h (10–15 neurospheres/well in 12-well low-binding plates). These neurospheres were stained with Annexin V and observed with a microscope, as mentioned above. GFP-Tg mice were purchased from CLEA Japan Inc.

Administration of GITR–Ab or GITR–Fc. GITR–Ab (100 μg/mice, DTA-1; eBioscience), GITR–Fc fusion protein (6.25 μg/mice)[16] or rat IgG isotype control (100 μg/mice, eBioscience) was intraperitoneally administered to mice at 3 h and 3 days after stroke.

Administration of T cells into poststroke SCID mice. T cells (1×10^6 cells/100 μl in PBS) obtained from several strains of mice (stimulated or non-stimulated by GITR-Ab), including CB-17, GFP-Tg, Gld- or C57/B6 mice, were injected intravenously into SCID mice at 48 h after stroke. Mice were subjected to histological examination after stroke. In another experiment, their brains were utilized for PCR analysis of nestin and Sox2.

Statistical analysis. Results were reported as the mean standard deviation. Statistical comparisons among groups were determined using one-way analysis of variance. Where indicated, individual comparisons were performed using Student's *t*-test. The groups with $P<0.01$ or, in some cases, $P<0.05$ differences were considered significant.

Conflict of Interest

The authors declare no conflict of interest.

Acknowledgements. This work was partially supported by a Grant-in-Aid for Scientific Research from the Ministry of Education, Culture, Sports, Science and Technology (21590473), and Hyogo Science and Technology Association. We thank Y Okinaka and Y Tanaka for technical assistance, and Dr. H Yamamoto for helpful discussion.

1. Hurn P, Subramanian S, Parker S, Afentoulis M, Kaler L, Vandenbark A *et al.* T- and B-cell-deficient mice with experimental stroke have reduced lesion size and inflammation. *J Cereb Blood Flow Metab* 2007; **27**: 1798–1805.
2. Liesz A, Suri-Payer E, Veltkamp C, Doerr H, Sommer C, Rivest S *et al.* Regulatory T cells are key cerebroprotective immunomodulators in acute experimental stroke. *Nat Med* 2009; **15**: 192–199.
3. Lambertsen K, Gregersen R, Meldgaard M, Clausen B, Heibøl E, Ladeby R *et al.* A role for interferon-gamma in focal cerebral ischemia in mice. *J Neuropathol Exp Neurol* 2004; **63**: 942–955.
4. de Bilbao F, Arsenijevic D, Moll T, Garcia-Gabay I, Vallet P, Langhans W *et al.* *In vivo* over-expression of interleukin-10 increases resistance to focal brain ischemia in mice. *J Neurochem* 2009; **110**: 12–22.
5. Arvidsson A, Collin T, Kirik D, Kokaia Z, Lindvall O. Neuronal replacement from endogenous precursors in the adult brain after stroke. *Nat Med* 2002; **8**: 963–970.
6. Nakagomi T, Taguchi A, Fujimori Y, Saino O, Nakano-Doi A, Kubo S *et al.* Isolation and characterization of neural stem/progenitor cells from post-stroke cerebral cortex in mice. *Eur J Neurosci* 2009; **29**: 1842–1852.
7. Taguchi A, Soma T, Tanaka H, Kanda T, Nishimura H, Yoshikawa H *et al.* Administration of CD34+ cells after stroke enhances neurogenesis via angiogenesis in a mouse model. *J Clin Invest* 2004; **114**: 330–338.
8. Saino O, Taguchi A, Nakagomi T, Nakano-Doi A, Kashiwamura S, Doe N *et al.* Immunodeficiency reduces neural stem/progenitor cell apoptosis and enhances neurogenesis in the cerebral cortex after stroke. *J Neurosci Res* 2010; **88**: 2385–2397.
9. Kleinschnitz C, Schwab N, Kraft P, Hagedorn I, Dreykluft A, Schwarz T *et al.* Early detrimental T-cell effects in experimental cerebral ischemia are neither related to adaptive immunity nor thrombus formation. *Blood* 2010; **115**: 3835–3842.
10. Yilmaz G, Arumugam T, Stokes K, Granger D. Role of T lymphocytes and interferon-gamma in ischemic stroke. *Circulation* 2006; **113**: 2105–2112.
11. Popovich PG, Longbrake EE. Can the immune system be harnessed to repair the CNS? *Nat Rev Neurosci* 2008; **9**: 481–493.
12. Nocentini G, Giunchi L, Ronchetti S, Krausz L, Bartoli A, Moraca R *et al.* A new member of the tumor necrosis factor/nerve growth factor receptor family inhibits T cell receptor-induced apoptosis. *Proc Natl Acad Sci USA* 1997; **94**: 6216–6221.
13. Shimizu J, Yamazaki S, Takahashi T, Ishida Y, Sakaguchi S. Stimulation of CD25(+)CD4(+) regulatory T cells through GITR breaks immunological self-tolerance. *Nat Immunol* 2002; **3**: 135–142.
14. Kwon B, Yu KY, Ni J, Yu GL, Jang IK, Kim YJ *et al.* Identification of a novel activation-inducible protein of the tumor necrosis factor receptor superfamily and its ligand. *J Biol Chem* 1999; **274**: 6056–6061.
15. Cuzzocrea S, Nocentini G, Di Paola R, Agostini M, Mazzon E, Ronchetti S *et al.* Proinflammatory role of glucocorticoid-induced TNF receptor-related gene in acute lung inflammation. *J Immunol* 2006; **177**: 631–641.
16. Nocentini G, Cuzzocrea S, Genovese T, Bianchini R, Mazzon E, Ronchetti S *et al.* Glucocorticoid-induced tumor necrosis factor receptor-related (GITR)-Fc fusion protein inhibits GITR triggering and protects from the inflammatory response after spinal cord injury. *Mol Pharmacol* 2008; **73**: 1610–1621.
17. Kohm A, Williams J, Miller S. Cutting edge: ligation of the glucocorticoid-induced TNF receptor enhances autoreactive CD4+ T cell activation and experimental autoimmune encephalomyelitis. *J Immunol* 2004; **172**: 4686–4690.
18. Gelderblom M, Leypoldt F, Steinbach K, Behrens D, Choe C, Siler D *et al.* Temporal and spatial dynamics of cerebral immune cell accumulation in stroke. *Stroke* 2009; **40**: 1849–1857.
19. Clausen BH, Lambertsen KL, Babcock AA, Holm TH, Dagnaes-Hansen F, Finsen B. Interleukin-1beta and tumor necrosis factor-alpha are expressed by different subsets of microglia and macrophages after ischemic stroke in mice. *J Neuroinflammation* 2008; **5**: 46.
20. Nakano-Doi A, Nakagomi T, Fujikawa M, Nakagomi N, Kubo S, Lu S *et al.* Bone Marrow mononuclear cells promote proliferation of endogenous neural stem cells through vascular niches after cerebral infarction. *Stem Cells* 2010; **28**: 1292–1302.
21. Nakagomi N, Nakagomi T, Kubo S, Nakano-Doi A, Saino O, Takata M *et al.* Endothelial cells support survival, proliferation, and neuronal differentiation of transplanted adult ischemia-induced neural stem/progenitor cells after cerebral infarction. *Stem Cells* 2009; **27**: 2185–2195.
22. Abematsu M, Tsujimura K, Yamano M, Saito M, Kohno K, Kohyama J *et al.* Neurons derived from transplanted neural stem cells restore disrupted neuronal circuitry in a mouse model of spinal cord injury. *J Clin Invest* 2010; **120**: 3255–3266.
23. Iosif R, Ekdahl C, Ahlenius H, Pronk C, Bonde S, Kokaia Z *et al.* Tumor necrosis factor receptor 1 is a negative regulator of progenitor proliferation in adult hippocampal neurogenesis. *J Neurosci* 2006; **26**: 9703–9712.
24. Muriglan SJ, Ramirez-Montagut T, Alpdogan O, Van Huystee TW, Eng JM, Hubbard VM *et al.* GITR activation induces an opposite effect on alloreactive CD4(+) and CD8(+) T cells in graft-versus-host disease. *J Exp Med* 2004; **200**: 149–157.
25. Schneider E, Moreau G, Arnould A, Vasseur F, Khodabaccus N, Dy M *et al.* Increased fetal and extramedullary hematopoiesis in Fas-deficient C57BL/6-lpr/lpr mice. *Blood* 1999; **94**: 2613–2621.
26. Zhan Y, Funda DP, Every AL, Fundova P, Purton JF, Liddicoat DR *et al.* TCR-mediated activation promotes GITR upregulation in T cells and resistance to glucocorticoid-induced death. *Int Immunol* 2004; **16**: 1315–1321.
27. Suvas S, Kim B, Sarangi PP, Tone M, Waldmann H, Rouse BT. *In vivo* kinetics of GITR and GITR ligand expression and their functional significance in regulating viral immunopathology. *J Virol* 2005; **79**: 11935–11942.
28. Monteiro RM, Camara NO, Rodrigues MM, Tzelepis F, Damião MJ, Cenedeze MA *et al.* A role for regulatory T cells in renal acute kidney injury. *Transpl Immunol* 2009; **21**: 50–55.
29. Cuzzocrea S, Nocentini G, Di Paola R, Mazzon E, Ronchetti S, Genovese T *et al.* Glucocorticoid-induced TNF receptor family gene (GITR) knockout mice exhibit a resistance to splanchnic artery occlusion (SAO) shock. *J Leukoc Biol* 2004; **76**: 933–940.
30. Ronchetti S, Zollo O, Bruscoli S, Agostini M, Bianchini R, Nocentini G *et al.* GITR, a member of the TNF receptor superfamily, is costimulatory to mouse T lymphocyte subpopulations. *Eur J Immunol* 2004; **34**: 613–622.
31. O'Garra A, Vieira P. Regulatory T cells and mechanisms of immune system control. *Nat Med* 2004; **10**: 801–805.
32. Meisel C, Schwab JM, Prass K, Meisel A, Dimagl U. Central nervous system injury-induced immune deficiency syndrome. *Nat Rev Neurosci* 2005; **6**: 775–786.
33. Zacharchuk CM, Meræep M, Chakraborti PK, Simons SS, Ashwell JD. Programmed T lymphocyte death. Cell activation- and steroid-induced pathways are mutually antagonistic. *J Immunol* 1990; **145**: 4037–4045.
34. Iosif R, Ahlenius H, Ekdahl C, Darsalia V, Thored P, Jovinge S *et al.* Suppression of stroke-induced progenitor proliferation in adult subventricular zone by tumor necrosis factor receptor 1. *J Cereb Blood Flow Metab* 2008; **28**: 1574–1587.
35. Hwang H, Lee S, Lee W, Lee H, Suk K. Stimulation of glucocorticoid-induced tumor necrosis factor receptor family-related protein ligand (GITRL) induces inflammatory activation of microglia in culture. *J Neurosci Res* 2010; **88**: 2188–2196.

36. Cantarella G, Di Benedetto G, Scollo M, Paterniti I, Cuzzocrea S, Bosco P *et al.* Neutralization of tumor necrosis factor-related apoptosis-inducing ligand reduces spinal cord injury damage in mice. *Neuropsychopharmacology* 2010; **35**: 1302–1314.
37. Corsini NS, Sancho-Martinez I, Laudenklos S, Glagow D, Kumar S, Letellier E *et al.* The death receptor CD95 activates adult neural stem cells for working memory formation and brain repair. *Cell Stem Cell* 2009; **5**: 178–190.
38. O' Reilly LA, Tai L, Lee L, Kruse EA, Grabow S, Fairlie WD *et al.* Membrane-bound Fas ligand only is essential for Fas-induced apoptosis. *Nature* 2009; **461**: 659–663.
39. Nocentini G, Ronchetti S, Cuzzocrea S, Riccardi C. GITR/GITRL: more than an effector T cell co-stimulatory system. *Eur J Immunol* 2007; **37**: 1165–1169.
40. Nishimura Y, Hirabayashi Y, Matsuzaki Y, Musette P, Ishii A, Nakauchi H *et al. In vivo* analysis of Fas antigen-mediated apoptosis: effects of agonistic anti-mouse Fas mAb on thymus, spleen and liver. *Int Immunol* 1997; **9**: 307–316.

Supplementary Information accompanies the paper on Cell Death and Differentiation website (http://www.nature.com/cdd)

Experimental Neurology 233 (2012) 481–489

Contents lists available at SciVerse ScienceDirect

Experimental Neurology

journal homepage: www.elsevier.com/locate/yexnr

Cerebral blood flow during reperfusion predicts later brain damage in a mouse and a rat model of neonatal hypoxic–ischemic encephalopathy

Makiko Ohshima [a], Masahiro Tsuji [a,*], Akihiko Taguchi [a], Yukiko Kasahara [a], Tomoaki Ikeda [a,b]

[a] Department of Regenerative Medicine and Tissue Engineering, National Cerebral and Cardiovascular Center Research Institute, 5-7-1, Fujishiro-dai, Suita, Osaka, 565-8565, Japan
[b] Department of Perinatology, National Cerebral and Cardiovascular Center Research Institute, 5-7-1, Fujishiro-dai, Suita, Osaka, 565-8565, Japan

ARTICLE INFO

Article history:
Received 12 September 2011
Accepted 11 November 2011
Available online 27 November 2011

Keywords:
Hypoxic–ischemic brain injury
Cerebral blood flow
Reperfusion
Laser speckle flowmetry
Neonatal
Rat
Mouse
Dexamethasone

ABSTRACT

Children with severe neonatal hypoxic–ischemic encephalopathy (HIE) die or develop life-long neurological impairments such as cerebral palsy and mental retardation. Decreased regional cerebral blood flow (CBF) is believed to be the predominant factor that determines the level of tissue injury in the immature brain. However, the spatio-temporal profiles of CBF after neonatal HIE are not well understood. CB17 mouse and Wistar rat pups were exposed to a unilateral hypoxic–ischemic (HI) insult at eight or seven days of age. Laser speckle imaging sequentially measured the cortical surface CBF before the hypoxic exposure and until 24 h after the hypoxic exposure. Seven days after the HI insult, brain damage was morphologically assessed by measuring the hemispheric volumes and by semi-quantitative scoring for neuropathologic injury. The mean CBF on the ipsilateral hemisphere in mice decreased after carotid artery ligation. After the end of hypoxic insult (i.e., the reperfusion phase), the mean CBF level gradually rose and nearly attained its pre-surgery level by 9 h of reperfusion. It then decreased. The degree of reduced CBF during reperfusion was well correlated with the degree of later morphological brain damage. The correlation was the strongest when the CBF was measured in the ischemic core region at 24 h of reperfusion in mice ($R^2 = 0.89$). A similar trend in results was found in rats. These results suggest that the CBF level during reperfusion may be a useful predictive factor for later brain damage in immature mice. This may enable optimizing brain damage for detail analyses.

Introduction

Children with severe neonatal hypoxic–ischemic encephalopathy (HIE) typically die or develop life-long neurological impairments such as cerebral palsy, mental retardation, and epilepsy (van Handel et al., 2007). No therapeutic method is available for perinatal HIE, apart from initiating hypothermia within 6 h after birth. An important issue in neonatal practice is the early detection of pathophysiological factors that are associated with permanent brain damage. Extensive laboratory research with experimental models is being performed to understand the mechanisms of brain injury and to find neuroprotective therapies. The Rice–Vannucci model, which combines permanent unilateral ligation of a carotid artery with exposure to hypoxia for 2 to 3 h in seven-day-old rat pups, has been widely used to study the physiological and therapeutic variables of neonatal hypoxic–ischemic (HI) injury (Johnston et al., 2005; Rice et al., 1981). This model has also been adapted for use in neonatal mice.

Decreased regional cerebral blood flow (CBF) is the predominant factor that determines the topography of tissue injury in the immature rodent brain, although metabolic factors (i.e., intrinsic vulnerability) may influence injury in some brain structures (Ringel et al., 1991; Vannucci et al., 1988). In immature rats with an HI injury, radioactive tracers in coronal sections show a residual columnar perfusion deficit within the cerebral cortex, which corresponds closely to the pathological pattern of injury within this structure. The pathological pattern of injury is characterized by alternating columns of normal and damaged neurons, which are oriented at a right angle to the pial surface. CBF is rarely monitored during and after HI insult in immature rodent models, mainly because of the technical difficulties and invasiveness involved in measuring it. Therefore, little is known about the spatial and temporal extent of CBF response during the reperfusion period after an HI insult.

The autoradiographic techniques for analyzing CBF in small animals entail sacrificing the animals at the time of measurement. A less invasive method, laser Doppler flowmetry (LDF), has been widely used to monitor relative perfusion changes. The LDF technique uses a single-point measurement in which the hemodynamics of an area covering 1 mm^3 to 2 mm^3 can be measured from the tip of a probe (Stern et al., 1977). CBF measured at a small arbitrarily selected area may not accurately reflect the hemodynamics of the cerebral hemisphere, and the

Abbreviations: NHIE, neonatal hypoxic–ischemic encephalopathy; HI, hypoxic–ischemic, hypoxia–ischemia; CBF, cerebral blood flow; LSF, laser speckle flowmetry; LDF, laser Doppler flowmetry; ROI, region of interest; MCA, middle cerebral artery; MRI, magnetic resonance imaging; DWI, Diffusion-weighted MRI; ANOVA, analysis of variance.

* Corresponding author. Fax: +81 6 6835 5496.
E-mail addresses: oshimam@ri.ncvc.go.jp, mtsujimd@ybb.ne.jp (M. Ohshima), mtsuji@ri.ncvc.go.jp (M. Tsuji), taguchi@ri.ncvc.go.jp (A. Taguchi), kasahara@ri.ncvc.go.jp (Y. Kasahara), tikeda@hsp.ncvc.go.jp (T. Ikeda).

0014-4886/$ – see front matter © 2011 Elsevier Inc. All rights reserved.
doi:10.1016/j.expneurol.2011.11.025